

Master's Thesis  
석사 학위논문

Acrylate-based Gel Polymer Electrolyte Exhibiting Better  
Rate Performance than Liquid Electrolyte

Donghui Kim(김 동 휘 金 東 輝 )

Department of Energy Systems Engineering  
에너지시스템공학전공

DGIST

2013

Master's Thesis  
석사 학위논문

Acrylate-based Gel Polymer Electrolyte Exhibiting Better  
Rate Performance than Liquid Electrolyte

Donghui Kim(김 동 휘 金 東 輝 )

Department of Energy Systems Engineering  
에너지시스템공학전공

DGIST

2013

Acrylate-based Gel Polymer Electrolyte Exhibiting Better  
Rate Performance than Liquid Electrolyte

Advisor : Professor 이 호 춘

Co-advisor : Doctor 김 재 현

by

김 동 휘

Department of Energy Systems Engineering  
DGIST

A thesis submitted to the faculty of DGIST in partial fulfillment of the requirements for the degree of Master of Science. The study was conducted in accordance with Code of Research Ethics<sup>1</sup>

11. 15. 2012

Approved by

Professor 이 호 춘 ( Signature )  
(Advisor)

Doctor 김 재 현 ( Signature )  
(Co-Advisor)

---

<sup>1</sup> Declaration of Ethical Conduct in Research: I, as a graduate student of DGIST, hereby declare that I have not committed any acts that may damage the credibility of my research. These include, but are not limited to: falsification, thesis written by someone else, distortion of research findings or plagiarism. I affirm that my thesis contains honest conclusions based on my own careful research under the guidance of my thesis advisor.

Acrylate-based Gel Polymer Electrolyte Exhibiting Better  
Rate Performance than Liquid Electrolyte

김 동 휘

Accepted in partial fulfillment of the requirements for the de-  
gree of Master of Science

11. 15. 2012

Head of Committee \_\_\_\_\_ (인)

Prof. 이 호 춘

Committee Member \_\_\_\_\_ (인)

Dr. 김 재 현

Committee Member \_\_\_\_\_ (인)

Prof. 홍 승 태

MS/ES  
201124002

김 동 휘. Donghui Kim. Acrylate-based Gel Polymer Electrolyte Exhibiting Better Rate Performance than Liquid Electrolyte. Department of Energy Systems Engineering. 2013. 20p. Advisors Prof. Hochun Lee, Co-Advisors Dr. Jaehyun Kim

### ABSTRACT

Gel polymer electrolytes (GPEs) exhibit enhanced safety and dimensional stability over liquid electrolytes (LEs), which is the critical advantage for the application of the Li-ion batteries (LIBs) to the electric vehicles and the renewable energy storage. The LIBs employing GPEs, however, are known to suffer from inferior power density due to the poor ionic conductivity of GPEs compared with LEs. In this study, it is demonstrated that the acrylate-based GPEs, prepared by the in-situ thermal cross linking polymerization, can show higher power density than LEs. It is found that  $\text{LiNi}_{1/3}\text{Mn}_{1/3}\text{Co}_{1/3}\text{O}_2$ /graphite cell employing the GPE exhibits 60 % higher discharge capacity at 2 C rate than the cell with LEs. To reveal the reason for the improved power performance of the GPE, the charge transport behavior of the electrode/electrolyte interface is examined by using electrochemical impedance spectroscopy (EIS) at various temperatures. The activation energy of the GPE cell determined from the Arrhenius plot is lower than that of the LE cell, which is ascribed to the decreased desolvation energy of  $\text{Li}^+$  ion in the GPE. The effects of the types of cathode materials ( $\text{LiCoO}_2$ ,  $\text{LiNi}_{0.5}\text{Co}_{0.2}\text{Mn}_{0.3}\text{O}_2$ ) and separator (dry vs. wet) on the power performance of the GPE are also investigated.

Keywords: Li-ion batteries, Gel polymer electrolyte, Power performance, Solvation energy

# Contents

Abstract	i
List of contents	ii
List of tables	iv
List of figures	v
I . INTRODUCTION	
. . . . .	1
II . THEORITICAL BACKGROUND	
2.1 Type of electrolyte	
2.1.1 Liquid electrolyte(LE)	2
2.1.2 Solid electrolyte(SE)	3
2.1.3 Gel polymer electrolyte(GPE)	4
2.2 Overpotentials in LIBs	4
2.3 De-solvation energy	5
2.4 Electrochemical impedance spectroscopy(EIS) in battery field	6
III . EXPERIMENTAL	
3.1 Optimization of polymerization condition	7
3.2 Preparation of coin cell	8
3.3 Coin half/full cell assembly	9
3.4 Coin symmetric cell assembly	11
3.5 Coin cell rate performance test	11
3.6 Electrochemical impedance spectroscopy (EIS)	11
IV . RESURT AND DISCUSSION	
4.1. Optimization of polymerization condition for non free liquid	12
4.2. $\text{LiNi}_{1/3}\text{Co}_{1/3}\text{Mn}_{1/3}\text{O}_2$ /Graphite coin full cell test	13
4.3. $\text{LiNi}_{1/3}\text{Co}_{1/3}\text{Mn}_{1/3}\text{O}_2$ and Graphite Coin half cell test	

4.3.1 LiNi <sub>1/3</sub> Co <sub>1/3</sub> Mn <sub>1/3</sub> O <sub>2</sub> /lithium foil cell . . . . .	15
4.3.2 Graphite/lithium foil cell . . . . .	17
4.4. LiNi <sub>1/3</sub> Co <sub>1/3</sub> Mn <sub>1/3</sub> O <sub>2</sub> /Graphite coin full cell EIS test . . . . .	19
4.5. LiNi <sub>1/3</sub> Co <sub>1/3</sub> Mn <sub>1/3</sub> O <sub>2</sub> /LiNi <sub>1/3</sub> Co <sub>1/3</sub> Mn <sub>1/3</sub> O <sub>2</sub> coin symmetric cell EIS test	23
4.6. Effect of rate performance of separator type using LiNi <sub>1/3</sub> Co <sub>1/3</sub> Mn <sub>1/3</sub> O <sub>2</sub> and Graphite . . . . .	26
4.7. LiNi <sub>0.5</sub> Co <sub>0.2</sub> Mn <sub>0.3</sub> O <sub>2</sub> /Graphite and LiCoO <sub>2</sub> /Graphite coin full cell test using two type separators . . . . .	28
 V. CONCLUSION . . . . .	 30

## Tables

Table 1. Characteristics of organic solvent

Table 2. Characteristics of lithium salt

Table 3. Type of inorganic solid electrolyte

Table 4. Conditions of polymerization experiment

Table 5. Electrodes of each type coin cell

Table 6. Amount of free liquid after polymerization

Table 7. Specific discharge capacity of each rate of  $\text{LiNi}_{1/3}\text{Co}_{1/3}\text{Mn}_{1/3}\text{O}_2$ /Graphite coin full cell

Table 8. Specific discharge capacity of each rate of  $\text{LiNi}_{1/3}\text{Co}_{1/3}\text{Mn}_{1/3}\text{O}_2$ /lithium foil coin cell

Table 9. Specific discharge capacity of each rate of Graphite/lithium foil coin cell

## Figures

- Fig 1. Mechanism of lithium ion moving in polymer solid electrolyte
- Fig 2. Factor of overpotentials in LIBs discharge profile
- Fig 3. Schematic illustration of de-solvation energy at electrode and electrolyte interface
- Fig 4. Mechanism of activation energy of normal electrode and polymer coating electrode
- Fig 5. Nyquist plot and equivalent circuit of battery
- Fig 6. Schematic illustration of respective internal resistances at electrodes and electrolyte interface
- Fig 7. Schematic illustration of impedance in symmetric cell
- Fig 8. Structure of a) dipentaerythritol pentaacrylate/hexaacrylate b) ,5-dimethyl-2,5-di-(2-ethylhexanoyl peroxy) hexane
- Fig 9. An illustration of 2032 coin type cell
- Fig 10. Mechanism of thermal polymerization of acrylate monomer using peroxide initiator
- Fig 11. Photographs of each polymerization sample
- Fig 12. Liquid type and gel type  $\text{LiNi}_{1/3}\text{Co}_{1/3}\text{Mn}_{1/3}\text{O}_2$ /Graphite coin full cell a) discharge capacity at each rate, b) 0.5C and 2.0C-rate charge/discharge profile, and c) ratio of discharge capacity
- Fig 13. Liquid type and gel type  $\text{LiNi}_{1/3}\text{Co}_{1/3}\text{Mn}_{1/3}\text{O}_2$ /lithium foil coin cell a) discharge capacity at each rate, b) 0.5C and 2.0C-rate charge/discharge profile, and c) ratio of discharge capacity
- Fig 14. Liquid type and gel type Graphite/ lithium foil coin cell a) discharge capacity at each rate, b) 0.5C and 2.0C-rate charge/discharge profile, and c) ratio of discharge capacity
- Fig 15. Temperature dependence of EIS data with coin full cell before cycling, a) liquid electrolyte coin cell, and b) gel electrolyte coin cell
- Fig 16. Temperature dependence of interfacial resistance of coin full cell GPE and Liquid electrolyte before cycling
- Fig 17. Temperature dependence EIS data of coin full cell after cycling, a) liquid electrolyte coin cell, and b) gel electrolyte coin cell
- Fig 18. Temperature dependence of interfacial resistance of coin full cell GPE and Liquid electrolyte after all cycling
- Fig 19. Temperature dependence of EIS data with coin symmetric cell, a) liquid-liquid, b) liquid-gel, c) gel-liquid, and d) gel-gel
- Fig 20. Temperature dependence of interfacial resistance of coin cathode symmetric cell GPE and Liquid electrolyte

Fig 21. The  $\text{LiNi}_{1/3}\text{Co}_{1/3}\text{Mn}_{1/3}\text{O}_2$ /lithium foil coin cell discharge capacity at each rate a) Celgard C500, b) Celgard 2320, c) Tonen, and d) Asahi ND420

Fig 22. The  $\text{LiNi}_{1/3}\text{Co}_{1/3}\text{Mn}_{1/3}\text{O}_2$ /Graphite coin cell discharge capacity at each rate a) Tonen, and b) Celgard 2320

Fig 23. The  $\text{LiNi}_{0.5}\text{Co}_{0.2}\text{Mn}_{0.3}\text{O}_2$ /Graphite coin cell discharge capacity at each rate a) Tonen, and b) Celgard 2320

Fig 24. The  $\text{LiCoO}_2$ /Graphite coin cell discharge capacity at each rate a) Tonen, and b) Celgard 2320

# I . INTRODUCTION

The lithium ion batteries (LIBs) has been used in many electronic devices, especially portable device which needs no external power supply such as laptop and mobile phone. Furthermore, LIB has had hard time being adopted as a power source of instruments such as electric vehicle (EV) and energy storage system since battery system can store and provide energy whenever we need it. Although LIB can be used in portable device currently, battery still cannot be a candidate for such instruments because of low capacity, poor rate performance, and safety problem for large scale applications. Plenty of researches have been undertaken to achieve those requirements.

In particular, safety and long term stability is more important, due to the problems which from accidents like explosions and from the cost to replace battery. Many studies have done to use polymer for electrolyte part to improve safety and long term stability. The case of the cell with semi-interpenetrating network type GPE showed higher overcharge stability than LE.<sup>1</sup> When the general capacity is 100%, while LE was rapidly increased its temperature and the cell voltage to 150%, GPE plateau to 300% overcharge. In case of long term stability, Using GPE with poly(acrylonitrile-co-methyl methacrylate) matrix, discharge capacity was higher than LE after 50 cycles.<sup>2</sup> When high voltage 4.4V cycle performance was tested using poly(vinylidene fluoride (PVDF) GPE, GPE maintained more than 80% of the capacity after 500 cycles, while LE was 80% after 200 cycle. Also, at high temperature of 90°C, the thickness change were 0.11mm with GPE and 1.14mm with LE.<sup>3</sup>

Despite of these advantages, GPE cannot be widely used because of its lower rate performance than LE due to the low ionic conductivity. GPE with poly[ethyleneoxide-co-2-(2-methoxyethoxy)ethyl glycidyl ether-co-allyl glycidyl ether] had 60% of LE capacity at 5C-rate.<sup>4</sup> Therefore, the further research were coating ionic liquid, ceramic or other material to improve its ionic conductivity. Doping nano-Al<sub>2</sub>O<sub>3</sub> GPE showed better rate performance than non doping GPE.<sup>5</sup>

In this paper, gel polymer electrolyte (GPE) is successfully synthesized by in-situ thermal polymerization used

acrylate based monomer and peroxide based initiator instead of coating the electrode surface. Eventhough this GPE decreases ionic conductivity, the rate performace is higher than that of liquid electrolyte (LE). To verify the effects of gel type electrolyte, rate performance with different discharge rate is examined, and electro-chemical impedance spectroscopy (EIS) has been introduced to measure the internal impedance of cells.

## II. THEORITICAL BACKGROUND

### 2.1. Type of electrolyte

#### 2.1.1. Liquid electrolyte (LE)

In general, LE which is a mixture of solvent and Lithium salt is used for LIBs. Organic solvent is classified into two types. Ethylene carbonate (EC) and propylene carbonate (PC) are cyclic carbonate, and dimethyl carbonate (DMC), diethyl carbonate (DEC), and ethyl-methyl carbonate (EMC) are linear carbonate. Each carbonate has unique characteristics. For example, cyclic carbonate has not only high dielectric constant, but also high viscosity. On the other hand, linear carbonate has low dielectric constant, but has low viscosity. Thus, cyclic and linear carbonates are usually mixed to be optimized in dielectric constant and viscosity. Table 1 shows the characteristics of well-known organic solvents.

Organic solvent	m.w	m.p(°C)	b.p(°C)	electric constant	viscosity(cp)
Ethylene carbonate (EC)	88	36.4	248	89.6	1.92
Ppropylene carbonate (PC)	102	-49.2	242	64.4	2.53
Dimethyl carbonate (DMC)	90	0.5	90.2	3.1	0.59
Ethyl methyl carbonate (EMC)	104	-53	110	2.96	0.65
Diethyl carbonate (DEC)	118	-43.0	126	2.8	0.75

Table 1. Characteristics of organic solvent<sup>6</sup>

There are four widely used lithium salts, which are lithium perchlorate (LiClO<sub>4</sub>), lithium tetrafluoroborate

(LiBF<sub>4</sub>), lithium hexafluorophosphate (LiPF<sub>6</sub>), and bis(trifluoromethane)sulfonimide lithium salt (Li(CF<sub>3</sub>SO<sub>2</sub>)<sub>2</sub>N).

LiClO<sub>4</sub> is used for primary battery not for secondary battery due to safety problems, and LiBF<sub>4</sub> is used as an additive rather than salt because of its low ionic conductivity.<sup>7</sup> Since LiPF<sub>6</sub> has highest ionic conductivity among those well-known lithium salt, it is most widely used. However, LiPF<sub>6</sub> is so reactive on water which results in hydrofluoric acid generation that its can cause side reactions with electrode, and it also has poor thermal stability.<sup>8</sup> In case of Li(CF<sub>3</sub>SO<sub>2</sub>)<sub>2</sub>N, ionic conductivity and thermal stability are very good, but the problem is aluminum corrosion. Table 2 gives the characteristics of four lithium salts.<sup>9,10</sup>

	LiClO <sub>4</sub>	LiBF <sub>4</sub>	LiPF <sub>6</sub>	Li(CF <sub>3</sub> SO <sub>2</sub> ) <sub>2</sub> N
<b>Ionic conductivity</b>	○	△	○	○
<b>High temp. stability</b>	×	○	×	○
<b>Al corrosion</b>	○	○	○	×
<b>Cu corrosion</b>	○	○	○	○

Table 2. Characteristics of lithium salt

Using additives can be useful to achieve better ionic conductivity, lifetime, and stability for LE. Some additives such as vinylene carbonate (VC) assist forming more stable SEI layer, and other additives help over-charge problem to use redox shuttles or passivation layer contribute.<sup>11-14</sup>

### 2.1.2. Solid electrolyte (SE)

SE is divided into polymer SE and inorganic SE. SE commonly has higher stability, but lower ionic conductivity. Polymer SE consists of polymer and salt, the coordinate-bond among polymer can make lithium ions move.<sup>15-16</sup>

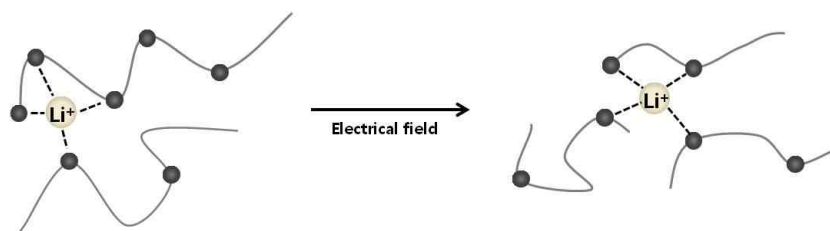


Fig 1. Mechanism of lithium ion moving in polymer solid electrolyte<sup>16</sup>

Inorganic SE such as LiPON has low ionic conductivity, but it is used for thin film battery.

Inorganic solid electrolyte	Conductivity (S/cm)
$\text{Li}_{2.9}\text{PO}_{3.3}\text{N}_{0.46}$ (LiPON)	$3.3 \times 10^{-6}$
$[\text{Li}_{1+x}\text{Ti}_2\text{Si}_x\text{P}_{3-x}\text{O}_{12}]$ -AIPO	$> 10^{-3}$
$(100-x)(0.6\text{Li}_2\text{S} \cdot 0.4\text{SiS}_2) \cdot x\text{Li}_4\text{SiO}_4$	$> 10^{-4}$
$\text{Li}_2\text{S-GeS}_2\text{-P}_2\text{S}_5$	$2.2 \times 10^{-3}$

Table 3. Type of inorganic solid electrolyte<sup>17-20</sup>

### 2.1.3. Gel polymer electrolyte (GPE)

GPE is comprised of polymer, organic solvent, and lithium salt. Since GPE is made by impregnating organic electrolyte into polymer matrix, it has moderate stability and ionic conductivity. All solvents and lithium salt for LE can be also used for GPE, and all polymers which can form matrix by crosslinking can be used for GPE. Generally, oxide, acrylonitrile, vinylene, and acrylate based polymers are frequently used.<sup>21-23</sup>

After finishing polymerization, if monomer remains in the electrolyte too much performance of the cell decreases.<sup>24-53</sup> Coating methods such as active material coating, electrode surface coating, and separator coating are frequently introduced to optimize the performance of GPE. Many kinds of polymer are used as coating materials. Thus, rate performance, long term stability, and thermal stability can be improved by coating methods.<sup>26-28</sup>

### 2.2. Overpotentials in LIBs

LIB has three types of overpotential: ohmic overpotential, activation overpotential, and concentration overpotential. Each factor of overpotential are IR drop, activation polarization, and concentration polarization. IR drop is the resistance of the bulk electrolyte when lithium ion move into electrolyte. Activation polarization is resistance of lithium ion intercalation or deintercalation. Concentration polarization occurred concentration of lithium ions decreases when while lithium ion is entering the electrode from surroundings due to migration.

Fig 2 is 0.5C and 1.5C-rate profile of the same cell. Cell discharge capacity is decreased due to increase in overpotential at high c-rate. This is because IR drop is increased due to increasing current, activation polarization is increased by velocity of lithium ion intercalation or deintercalation, and concentration polarization is

increased by speed of lithium ion migration at near the electrode.

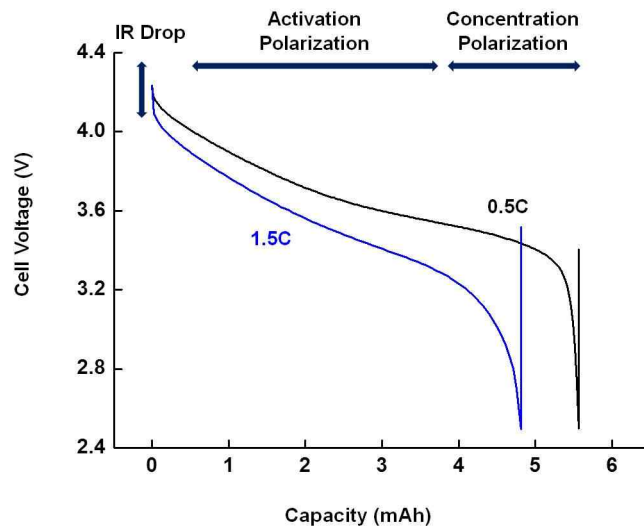


Fig 2. Factor of overpotentials in LIBs discharge profile

### 2.3. De-solvation energy

In the electrolyte, dissolved lithium ions move in coupled form with carbonate groups via coordinate bond. After lithium ions reach near the electrode surface, the bond should be eliminated so that Li ions are intercalated into the electrode. At this moment, activation energy for removing the bond is needed as shown in Fig 3. This energy is called de-solvation energy.<sup>29-30</sup>

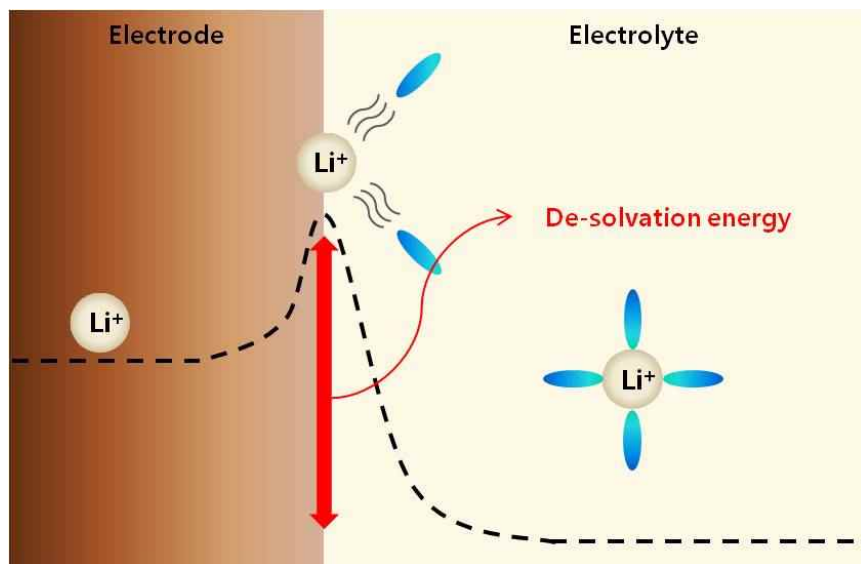


Fig 3. Schematic illustration of de-solvation energy at electrode and electrolyte interface<sup>31</sup>

The de-solvation energy is occurred by intercalation of lithium ion and electrolyte couple into the electrode after their separation. As the surface of electrode is coated, the de-solvation energy decreases since the activation energy  $\Delta E$  is divided into the  $\Delta E_1$  and  $\Delta E_2$ . Namely, de-solvation occurs at the interface between polymer and electrolyte, not between electrode and electrolyte, and thereby the energy for lithium intercalation between polymer and electrode is only needed. If  $\Delta E_1$  is much bigger than  $\Delta E_2$ , then  $E_2$  becomes rate determining step (RDS). Otherwise,  $\Delta E_1$  becomes RDS. Thus, reactions in GPE is faster than those in LE since reactions related to  $\Delta E_1$  and  $\Delta E_2$  occur at the same time in LE (Fig 4).<sup>32</sup>

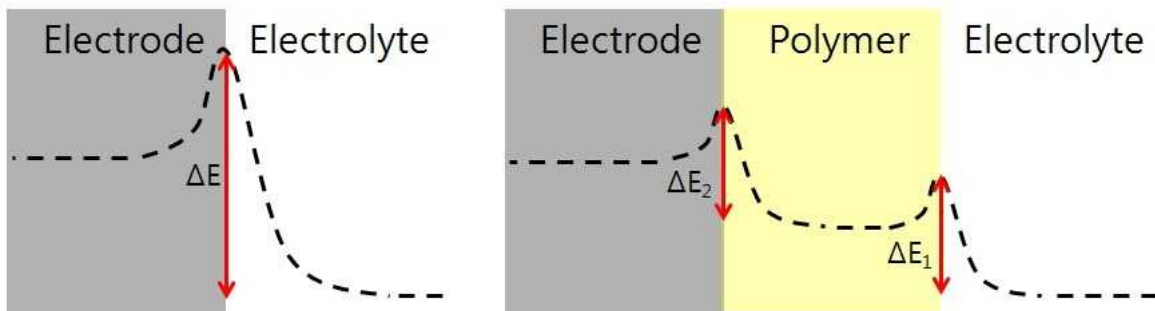


Fig 4. Mechanism of activation energy of normal electrode and polymer coating electrode<sup>32</sup>

#### 2.4. Electrochemical impedance spectroscopy (EIS) in battery field

Usual EIS data of battery is shown in Fig 5 The offset point of half-circle means  $R_b$  stands for resistance of electrolyte bulk. First semi circle includes multi-film resistance,  $R_{sei}$  because multi-film means solid electrolyte interface (SEI) layer. Second semi circle means charge transfer resistance,  $R_{ct}$  (Fig 5,6).<sup>33-34</sup>

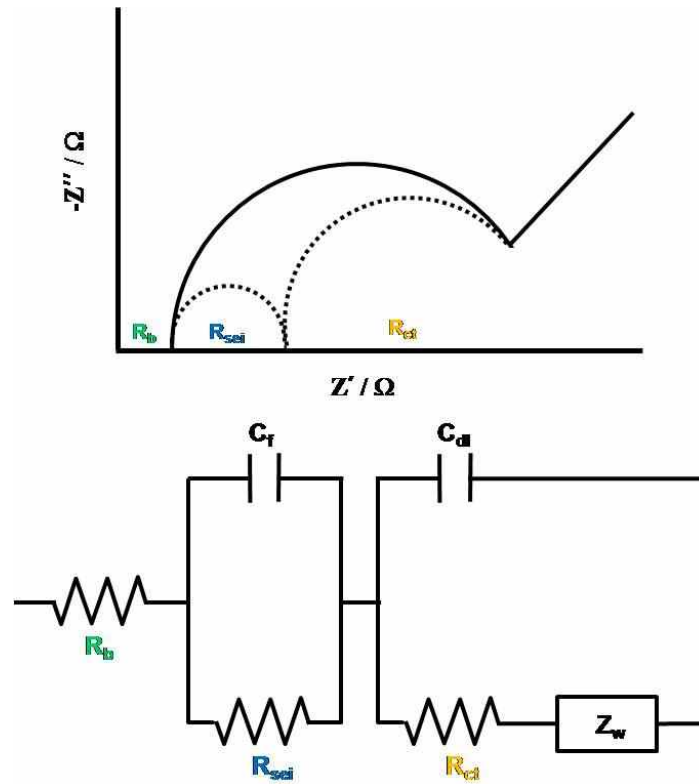


Fig 5. Nyquist plot and equivalent circuit of battery

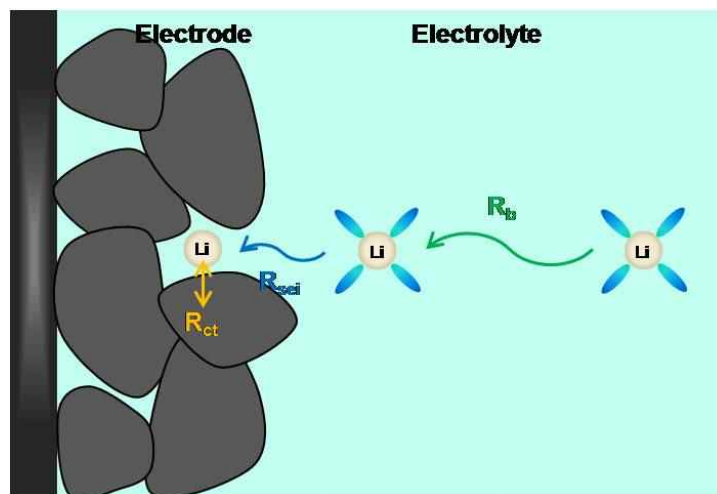


Fig 6. Schematic illustration of respective internal resistances at electrodes and electrlyte interface<sup>34</sup>

In case of the full cell EIS measurement, the reaction between cathode and anode can be observed.

However, it is difficult to examine the reaction on pure cathode side or anode side. To do so, half cell can be introduced, but it also cannot give us exact information because lithium foil which is reference and counter electrode of half cell might give influence on the EIS data. Thus, symmetric cell is introduced since it consists

of same active materials as a working electrode and reference and counter electrodes in a cell. Impedance of symmetric cell is written as  $2Z_+$  or  $2Z_-$  where  $Z$  means the impedance of one electrode side (Fig 7).<sup>34</sup> Therefore,  $Z$  can be obtained by taking half value of  $R_{sei}$  or  $R_{ct}$ .<sup>35-37</sup>

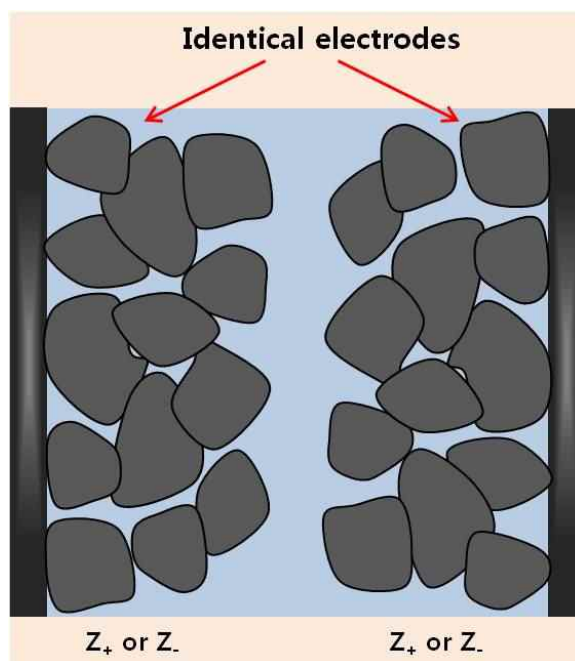


Fig 7. Schematic illustration of impedance in symmetric cell<sup>34</sup>

### III. Experimental

#### 3.1. Optimization of polymerization condition

3ml of electrolyte, monomer, and initiator solution are added in 4ml vial like the condition of the table 4. This vial is put in an oven and polymerization was conducted at 80°C. Fig 8a) is chemical structure of the monomer and Fig 8b) is chemical structure of the initiator.

Sample #	electrolyte	monomer	initiator	polymerization time	type of oven
①	1M LiPF <sub>6</sub> EC/EMC (1/2 vol%)	2wt% of electrolyte	2wt% of monomer	4hr	non vaccum oven
②		3wt% of electrolyte			
③	1M LiPF <sub>6</sub> EC/EMC (1/2 vol%)	5wt% of electrolyte	3wt% of monomer	4hr	non vaccum oven
④	1M LiPF <sub>6</sub> EC/EMC (1/2 vol%)	3wt% of electrolyte	2wt% of monomer	4hr	non vaccum oven
⑤			5wt% of monomer		
⑥	1M LiPF <sub>6</sub> EC/EMC (1/2 vol%)	3wt% of electrolyte	2wt% of monomer	4hr	vaccum oven
⑦	1M LiPF <sub>6</sub> EC/EMC (1/2 vol%)	2wt% of electrolyte	4wt% of monomer	3hr	vaccum oven

Table 4. Conditions of polymerization experiment

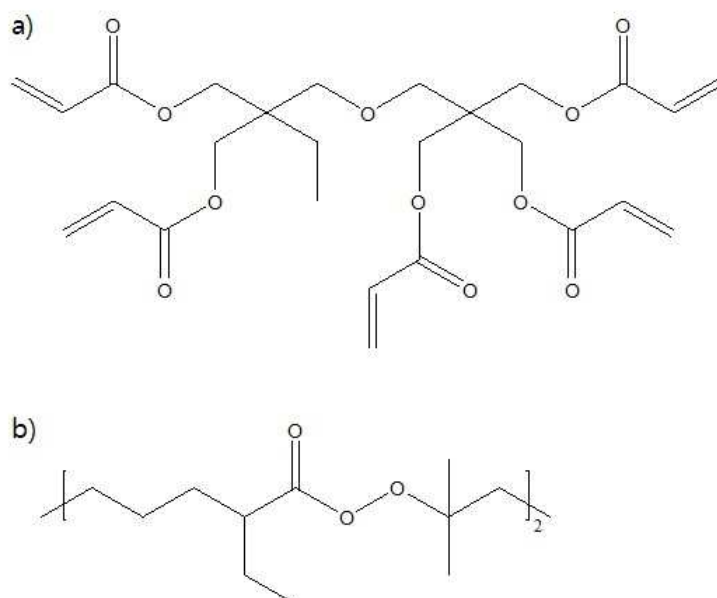


Fig 8. Structure of a) dipentaerythritol pentaacrylate/haxaacrylate b) ,5-dimethyl-2,5-di-(2-ethylhexanoyl peroxy) hexane

### 3.2. Preparation of coin cell

LiNi<sub>1/3</sub>Co<sub>1/3</sub>Mn<sub>1/3</sub>O<sub>2</sub>, LiNi<sub>0.5</sub>Co<sub>0.2</sub>Mn<sub>0.3</sub>O<sub>2</sub>, LiCoO<sub>2</sub>, and Graphite electrodes were punched in 14 mm diameter

disks from the large electrode strips using a punch. These were then dried under vacuum at 110 °C for at least 24 hours. Separators (Celgard C500, Celgard2320, Tonen, and Asahi ND420) were punched in 18 mm diameter disks and storage in glove box filled with argon. 1M LiPF<sub>6</sub> dissolved ethylene carbonate (EC) / Ethyl methyl carbonate (EMC) (1/2 by volume) solution was used as a LE. 1M LiPF<sub>6</sub> monomer (dipentaerythritol pentaacrylate/haxaacrylate, 2wt% of electrolyte), and initiator (2,5-dimethyl-2,5-di-(2-ethylhexanoyl peroxy) hexane, 4wt% of monomer) dissolved in EC / EMC (1/2 by volume) solution was used as GPE.

### 3.3. Coin half/full cell assembly

Coin cells are assembled by 2032 type. In order from the bottom of the Fig 9, 100µl of electrolyte was inject on the bottom case. After electrode (table 5) was placed, then a separator and a gasket were placed. Coin half cell case were to put more 100µl electrolyte and insert the lithium foil (16.15 mm diameter), 0.5 mm spacer, disk spring and top. Coin full cell cases were assembled with anode electrode and 1.0 mm spacer instead of lithium foil and 0.5 mm spacer. Lastly, coin cell sealed using clamping machine. After coin cell assembly, liquid type placed 20hr at 25°C for wetting. Gel type case were 6hr wetting at 25°C, polymerization at 80°C oven at 3hr, and 11hr wetting at 25 °C for wetting and cooling.

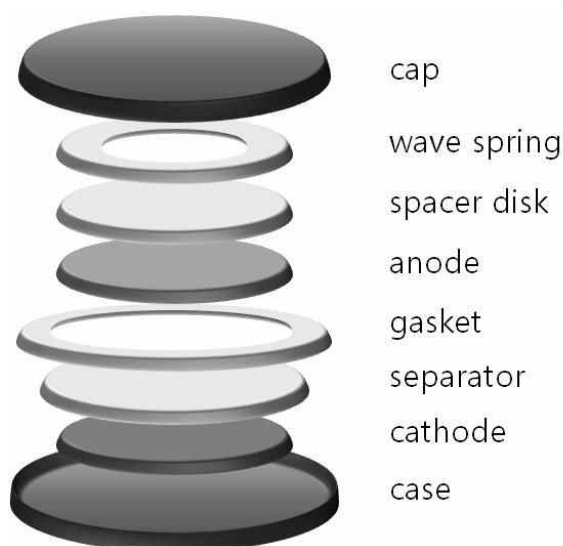


Fig 9. An illustration of 2032 coin type cell

Electrode	Half cell	Full cell	Symmetric cell
Cathode	$\text{LiNi}_{1/3}\text{Co}_{1/3}\text{Mn}_{1/3}\text{O}_2$ or graphite	$\text{LiNi}_{1/3}\text{Co}_{1/3}\text{Mn}_{1/3}\text{O}_2$	$\text{LiNi}_{1/3}\text{Co}_{1/3}\text{Mn}_{1/3}\text{O}_2$
Anode	Li foil	Graphite	$\text{LiNi}_{1/3}\text{Co}_{1/3}\text{Mn}_{1/3}\text{O}_2$

Table 5. Electrodes of each type coin cell

### 3.4. Coin symmetric cell assembly<sup>38</sup>

Half cells are assembled followed by 2 cycles in 0.2C to form the SEI layer. Then charge or discharge until one cell is zero percent state of charge (SOC0), and the other cell is one hundred percent state of charge (SOC100) with 0.2C rate and 1/20C cutoff condition. SOC0, and SOC100 half cell were disassembled and separate each electrode. To make symmetric cell, SOC100 electrode located at the bottom, and SOC0 electrode located at the top.

### 3.5 Coin cell rate performance test

TOSCAT-3100 (Toyo System Inc.) was used for all charge/discharge experiments. Constant current (CC) cut off condition was from 2.5V to 4.25V and constant voltage (CV) cut off condition was 1/20C. Experiments were conducted charge rate fixed 0.2C, and discharge rate increases from 0.2C to 4.0C putting 0.2C two recovery cycle in the intervals.

### 3.6. Electrochemical impedance spectroscopy (EIS)

Liquid/Gel type coin full/symmetric cell were prepared SOC0 after 0.2C three cycled. EIS measurement needed maintaining the voltage at 3.3V for 10min at different temperatures from 5°C to 45°C by 10°C intervals. EIS were measured from 1mHz to 200kHz at 5°C, from 5mHz to 200kHz at 15°C, and from 10mHz to 200kHz at other temperatures. EIS experiments progress using Biologic VSP model.

## IV. RESULT AND DISCUSSION

#### 4.1. Optimization of polymerization condition for non free liquid

Thermal polymerization of acrylate monomer using peroxide initiator easily removes O-O bond of peroxide by heat treatment, and thereby free radical is generated. Free radical is so reactive as to attack vinyl group of acrylate. Radical keeps moving and reacting until all monomers have been used (Fig 10).

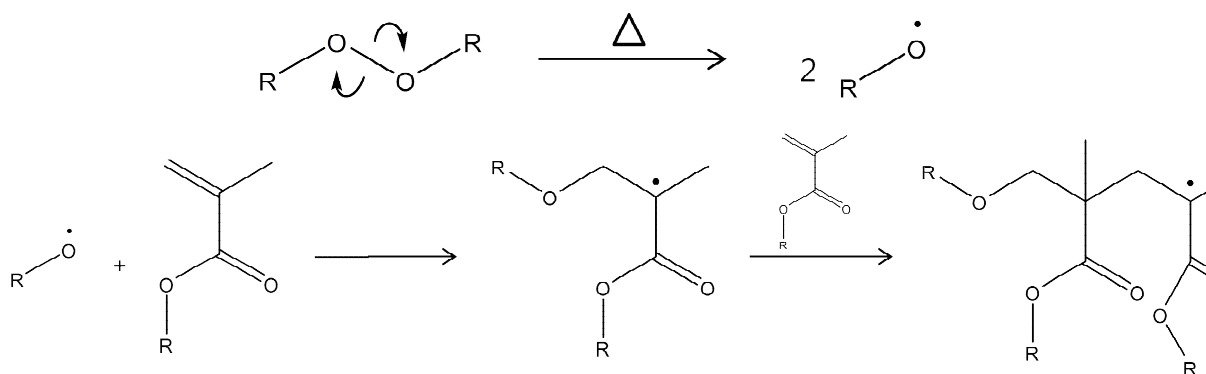


Fig 10. Mechanism of thermal polymerization of acrylate monomer using peroxide initiator

To find the condition of none free liquid using the minimum amount of monomer, experiments are conducted by adjusting the amount of monomer and initiator (Fig 11, and Table 6). As a result, it is found that free liquid remains when non vacuum oven is used.

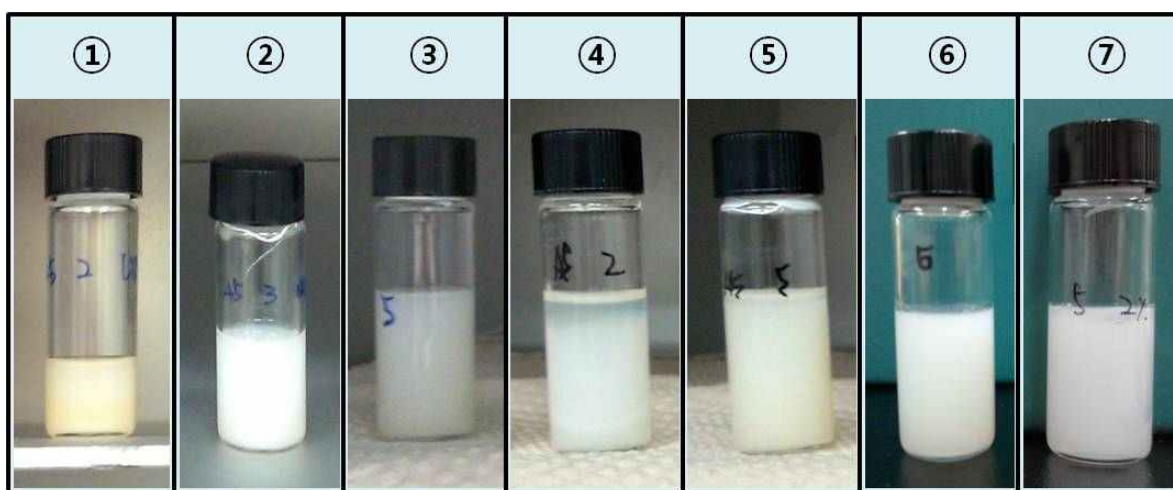


Fig 11. Photographs of each polymerization sample

Sample #	Amount of free liquid (height of liquid(mm))
①	1 mm
②	1 mm
③	0.5 mm
④	1 mm
⑤	0.5 mm
⑥	Non
⑦	Non

Table 6. Amount of free liquid after polymerization

Experiments were conducted using a vacuum oven to consider the effect of moisture or oxygen. The experimental in vacuum oven was no free liquid, in both cases (table 6). The coin cell assemble was decided seventh condition to consider problem cell placed in high temperature.

#### 4.2. $\text{LiNi}_{1/3}\text{Co}_{1/3}\text{Mn}_{1/3}\text{O}_2$ /Graphite coin full cell test

The rate performances of GPE and LE for various discharge rates are examined by coin full cell test. Fig 12a) shows discharge capacity of GPE and LE for different discharge rates. At the very beginning rate (0.2, 0.5C), the discharge capacity of GPE is lower, but it becomes much better than that of LE after 1.0C-rate. Fig 12b) gives charge/discharge profile at the first cycle 0.5C and 2.0C-rate. From this profile, the overpotential difference between GPE and LE is shown. In case of liquid type electrolyte, ohmic overpotential which stands for the decrement is always lower than that of GPE. Thus, it is found that gel polymer generated between electrodes causes resistance increment. Activation and concentration overpotential can be obtained by calculating the slope of profile curve. The slope in case of GPE is similar to that in case of liquid type electrolyte at low c-rate as shown in Fig 12b). However, as c-rate goes faster, the slope in case of GPE becomes gentle. This means that activation and concentration overpotential of GPE becomes small at high c-rate. Capacity ratio of both GPE and liquid type electrolyte is shown in Fig 12c). The ratio is based on the discharge rate of liquid type at 0.2C-rate. Table 7 represents discharge capacity for each rate. From those data, it is found that capacity and energy density of GPE becomes better than those of liquid type electrolyte at high c-rate due to decrease of overpotentials in case of GPE.

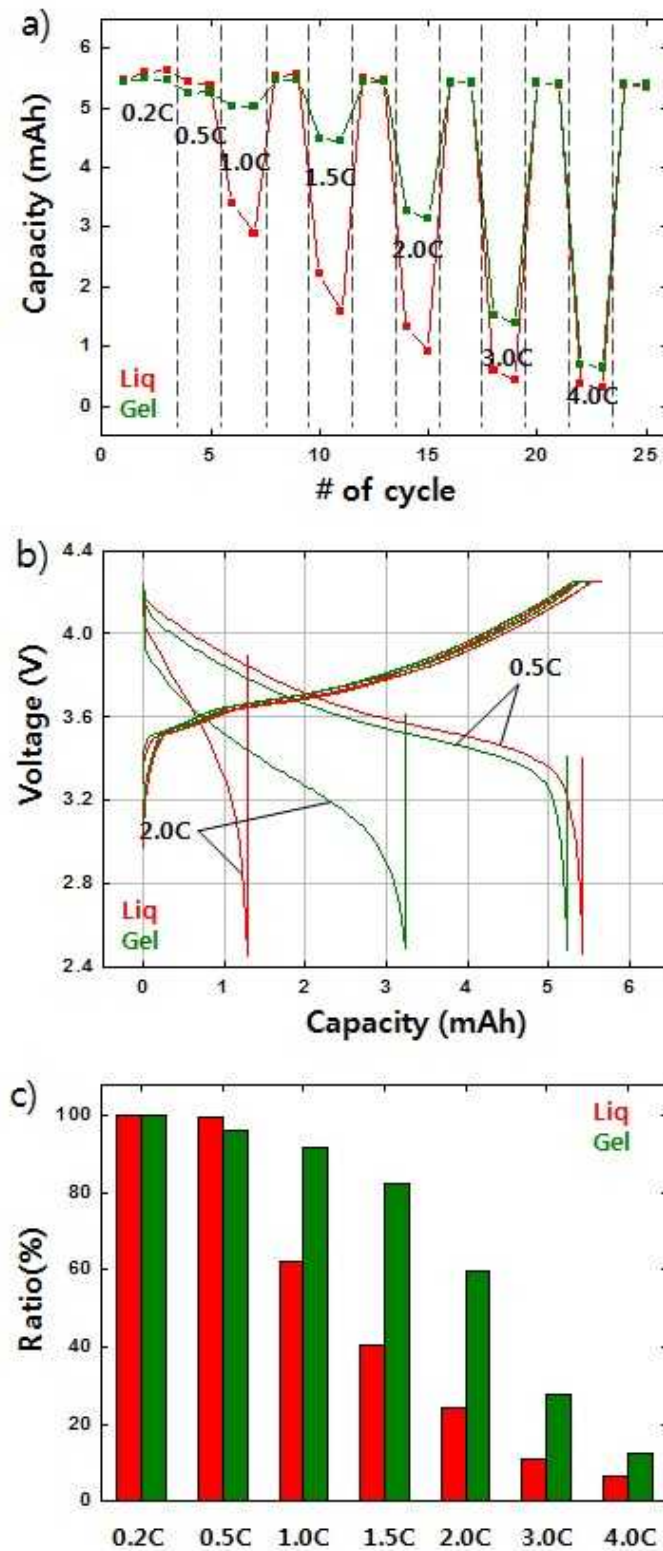


Fig 12. Liquid type and gel type  $\text{LiNi}_{1/3}\text{Co}_{1/3}\text{Mn}_{1/3}\text{O}_2/\text{Graphite}$  coin full cell a) discharge capacity at each rate, b) 0.5C and 2.0C-rate charge/discharge profile, and c) ratio of discharge capacity

		0.2C	0.5C	1.0C	1.5C	2.0C	3.0C	4.0C
Capacity (mAh)	Liq	5.463	5.434	3.395	2.217	1.315	0.588	0.355
	Gel	5.450	5.256	5.018	4.487	3.260	1.528	0.688

Table 7. Specific discharge capacity of each rate of  $\text{LiNi}_{1/3}\text{Co}_{1/3}\text{Mn}_{1/3}\text{O}_2$ /Graphite coin full cell

#### 4.3. $\text{LiNi}_{1/3}\text{Co}_{1/3}\text{Mn}_{1/3}\text{O}_2$ and Graphite Coin half cell test

Coin full cell test indicates that GPE has better rate performance at high c-rate. However, it is asked whether cathode mainly affects the rate performance or anode mainly does. Half cell test for each electrode material was undertaken to figure out which electrode material has much influence on rate performance.

##### 4.3.1. $\text{LiNi}_{1/3}\text{Co}_{1/3}\text{Mn}_{1/3}\text{O}_2$ /lithium foil cell

Fig 13a) gives discharge capacity of cathode half cell using both GPE and LE. As c-rate becomes faster the rate performance becomes better, which is somewhat similar to the results of coin full cell test. However, less difference between GPE and LE is observed at 1.0C-rate in comparison with data of coin full cell test. The cycle profile at the first cycle for 0.5C and 2.0C-rate is shown in Fig 13b). Ohmic overpotential is bigger than that of full cell test results, and it becomes much bigger at high c-rate. In case of activation and concentration overpotentials, both results of GPE are similar to those of liquid type electrolyte at low c-rate, respectively, but the resistance of GPE due to activation and concentration becomes less at high c-rate. Therefore, less difference in capacity at 1.0C as compared with data of coin full cell test is due to ohmic overpotential. Fig 13c) shows the discharge capacity ratio of cathode half cell test and table 8. also gives discharge capacity data just as coin full cell test.

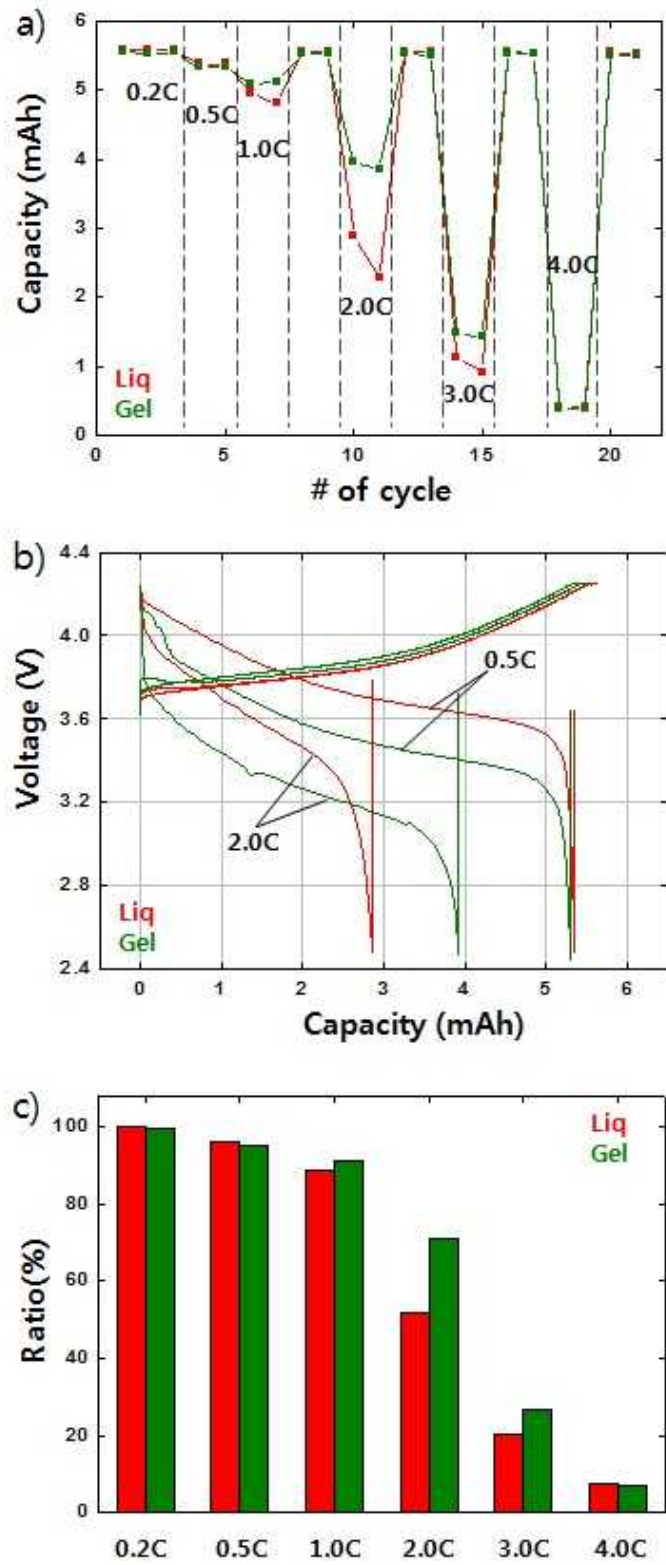


Fig 13. Liquid type and gel type  $\text{LiNi}_{1/3}\text{Co}_{1/3}\text{Mn}_{1/3}\text{O}_2$ /lithium foil coin cell a) discharge capacity at each rate, b) 0.5C and 2.0C-rate charge/discharge profile, and c) ratio of discharge capacity

		0.2C	0.5C	1.0C	2.0C	3.0C	4.0C
Capacity (mAh)	Liq	5.584	5.370	4.960	2.893	1.125	0.415
	Gel	5.546	5.320	5.086	3.956	1.491	0.388

Table 8. Specific discharge capacity of each rate of  $\text{LiNi}_{1/3}\text{Co}_{1/3}\text{Mn}_{1/3}\text{O}_2$ /lithium foil coin cell

#### 4.3.2. Graphite/lithium foil cell

The discharge capacity of anode half cell is shown in Fig 14a). On the anode side, discharge capacity of GPE is almost same as that of liquid type electrolyte. Fig 14b) which shows profile curves for examining effects of overpotentials indicates large ohmic overpotential is found during de-intercalation process of lithium ions in case of GPE. Plus, almost no constant voltage (CV) period is observed during intercalation process and rapid change in the slope of profile curve is monitored at the end of de-intercalation process. This leads to decrement of initial capacity which may be due to internal contact problem during gel polymerization process. Cycling tendency becomes usual after several cycles. The tendency of other overpotential is closely similar to each other. Fig 14c) also shows capacity ratio and table 9. gives discharge capacity data just as cathode half cell test.

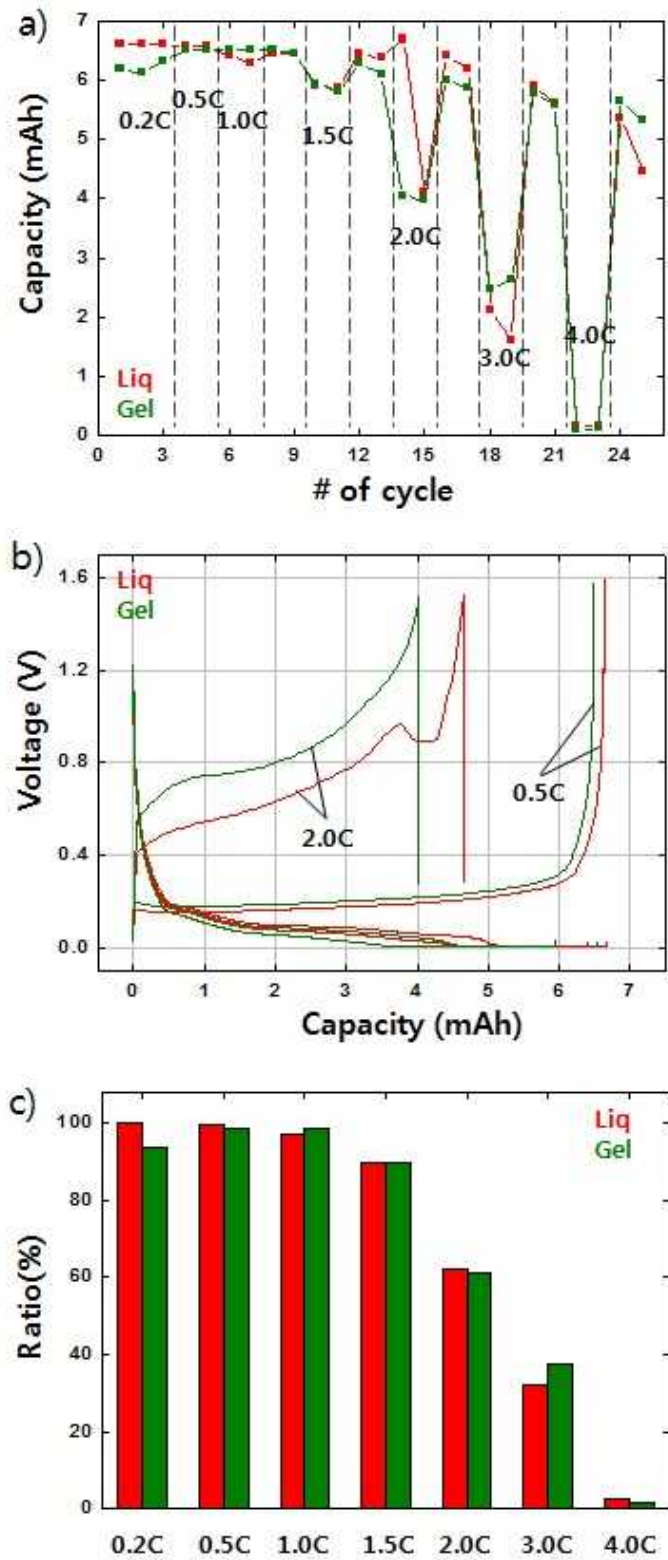


Fig 14. Liquid type and gel type Graphite/ lithium foil coin cell a) discharge capacity at each rate, b) 0.5C and 2.0C-rate charge/discharge profile, and c) ratio of discharge capacity

		0.2C	0.5C	1.0C	1.5C	2.0C	3.0C	4.0C
Capacity (mAh)	Liq	6.607	6.567	6.404	5.912	4.100	2.132	0.167
	Gel	6.177	6.506	6.495	5.934	4.050	2.466	0.110

Table 9. Specific discharge capacity of each rate of Graphite/ lithium foil coin cell

From the results of cathode and anode half cell test, it was found that ohmic overpotential in case of full cell in GPE is larger than that in case of half cell in GPE due to use of lithium foil as counter and reference electrode. Because of difference in the surface and reactivity between electrode active material and lithium foil, gel polymerization might become different from each other.

#### 4.4. $\text{LiNi}_{1/3}\text{Co}_{1/3}\text{Mn}_{1/3}\text{O}_2$ /Graphite coin full cell EIS test

In this paper, better rate performance was observed by conducting coin cell test using GPE. However, since GPE is usually known to have poor rate performance, the reason of conflicting results had to be explained. To examine the conflicting results, internal impedance was measured several times using EIS with respect to different temperature conditions so that de-solvation energy of lithium ions was obtained.

Fig 15a) and b) show EIS data of LE and GPE respectively. Impedance is measured after 3 cycles at the rate of 0.2C because SEI layer needs three cycles to be formed. Impedance of LE is higher at low temperature, and that of GPE is higher at high temperature.  $R_b$  of both LE and GPE is similar to each other, and is almost not a function of temperature.  $R_{sei}$  of LE is smaller than that of GPE and it is also not a function of temperature irrespective of the type of electrolyte.  $R_{ct}$  is sensitively changed by temperature, so its tendency is close to overall impedance. From this result,  $R_b$  is expected to have little difference since LE and GPE consist of same salt and solvent. The difference in  $R_{sei}$  between LE and GPE might be due to additional polymer layer in GPE.  $R_{ct}$  of GPE is different from that of LE because lithium ions intercalation process might be changed by polymer layer.

De-solvation energy of GPE and LE were obtained by calculating the slope of Arrhenius plot using  $R_{ct}$  value at various temperatures. De-solvation energy of GPE is smaller than that of LE as shown in Fig 16, and the reason why rate performance of GPE was better than that of LE was explainable from this result.

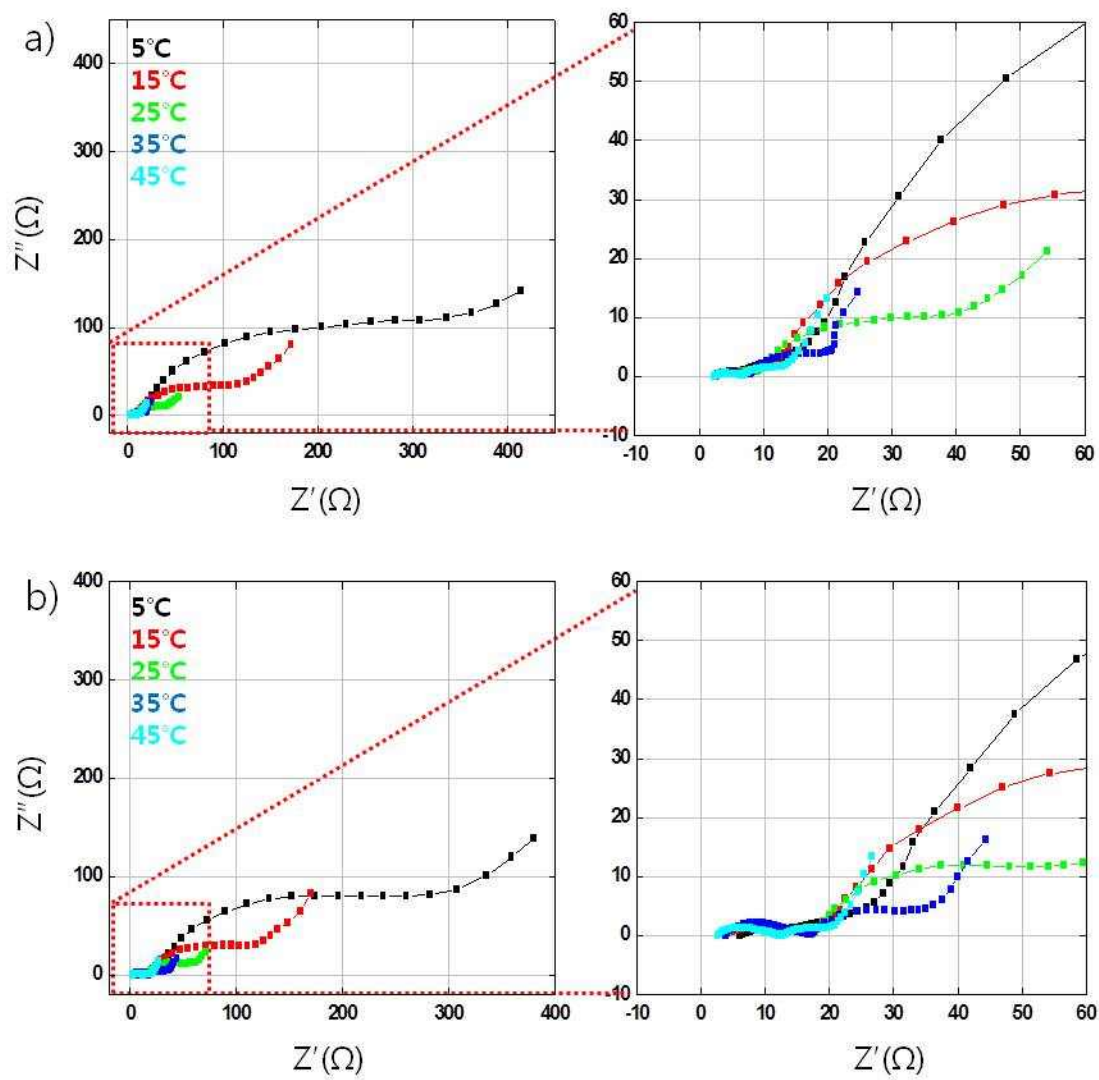


Fig 15. Temperature dependence of EIS data with coin full cell before cycling,

a) liquid electrolyte coin cell, and b) gel electrolyte coin cell

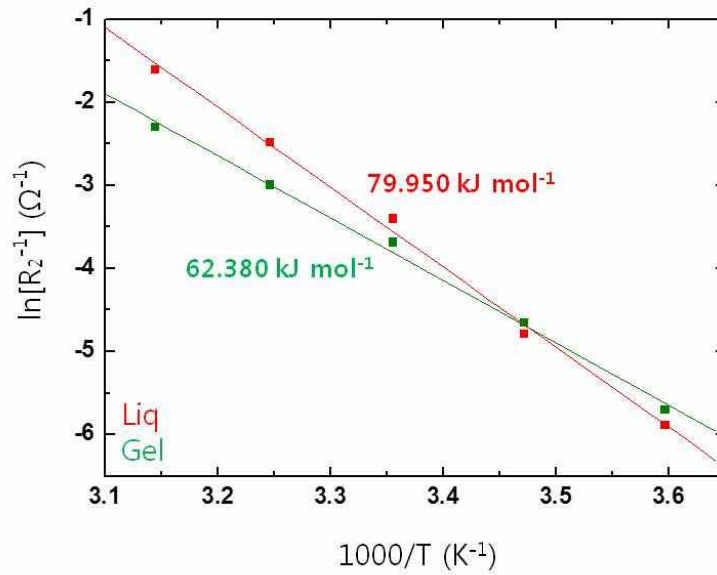


Fig 16. Temperature dependence of interfacial resistance of coin full cell  
GPE and Liquid electrolyte before cycling

Fig 17 shows the EIS data after rate performance test. LE and GPE resistance relatively compared at Fig 16, because of other cell used. The difference in the value of  $R_{ct}$  becomes much larger after cycling. Also, desolvation energies from the EIS data after cycling test become more different between LE and GPE (Fig 18). This is due to the damage caused by high rate discharge. In this measurement, the value of  $R_b$  was set to zero because the value of  $R_b$  cannot be compensated as temperature varies.

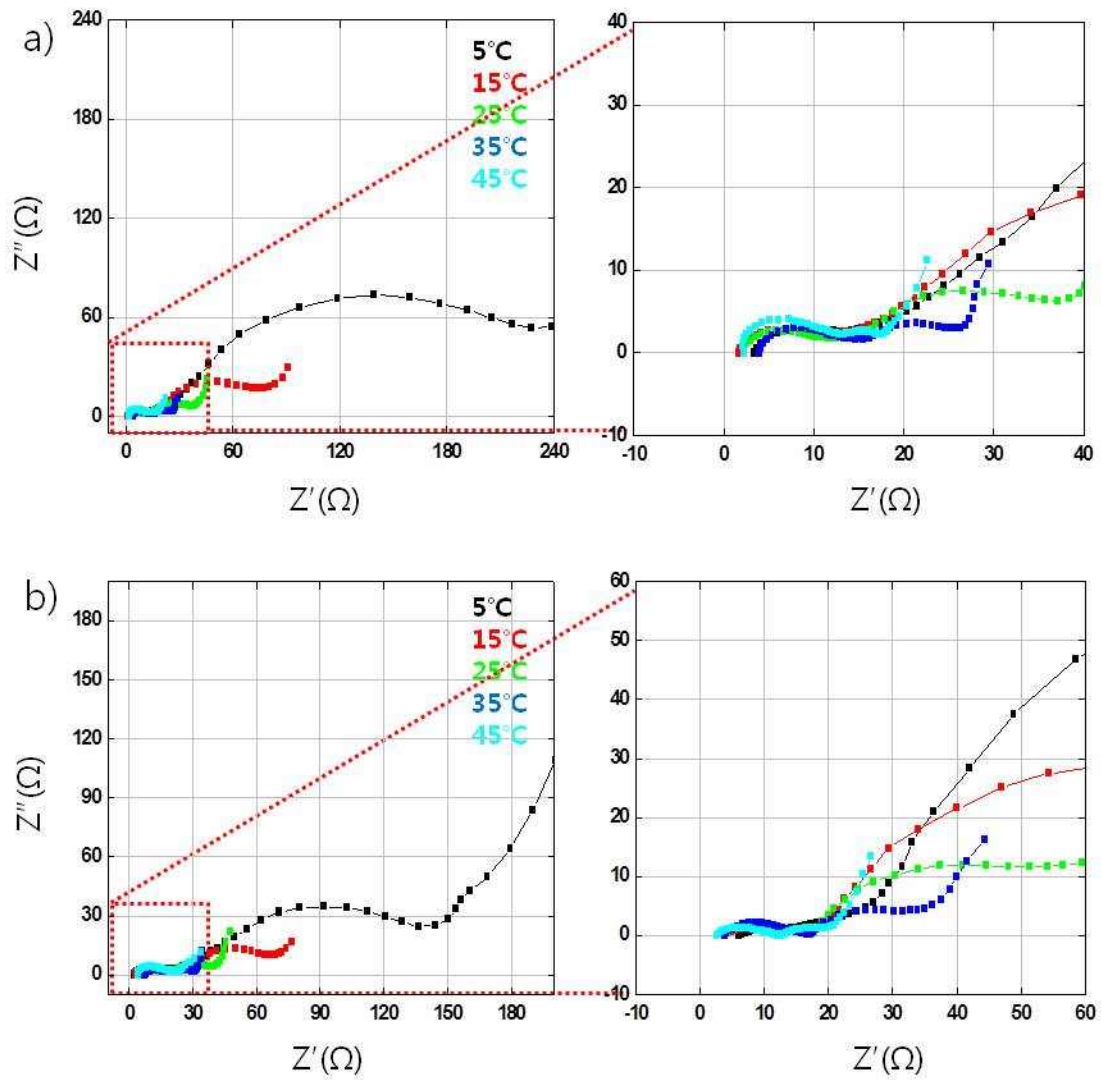


Fig 17. Temperature dependence EIS data of coin full cell after cycling,

a) liquid electrolyte coin cell, and b) gel electrolyte coin cell

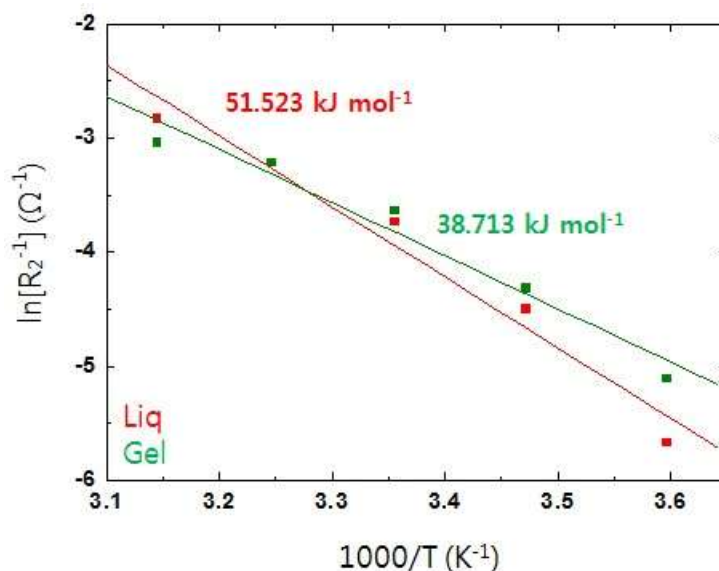


Fig 18. Temperature dependence of interfacial resistance of coin full cell  
GPE and Liquid electrolyte after all cycling

#### 4.5. LiNi<sub>1/3</sub>Co<sub>1/3</sub>Mn<sub>1/3</sub>O<sub>2</sub>/ LiNi<sub>1/3</sub>Co<sub>1/3</sub>Mn<sub>1/3</sub>O<sub>2</sub> coin symmetric cell EIS test

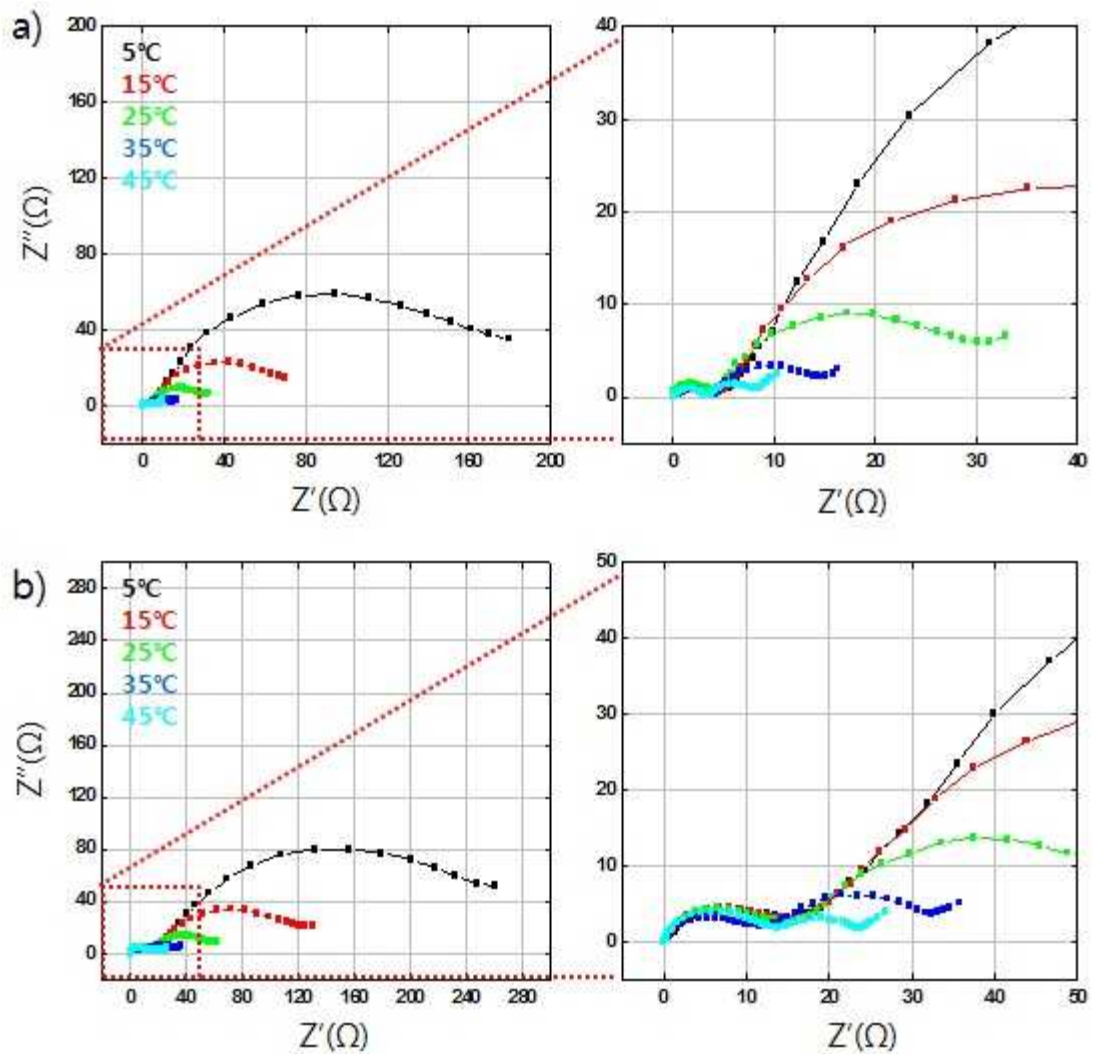
It was found that discharge capacity is mainly affected by cathode material rather than anode material. Thus, more sophisticated experiments focus on cathode material was EIS studied by measurement using symmetric cell. Symmetric cell which is charged and discharged by adjusting only state of charge (SOC) consists of either cathode materials or anode materials for all of the working electrode, reference electrode, and counter electrode. Since lithium foil is not used as an electrode in symmetric cell method, effect of side reactions due to lithium foil is eliminated, and thereby we could interpret the pure influence of active materials.

Two types (LE and GPE) of cells exist when the cells are assembled both in half cells and in symmetric cells. In the end, there are four cases of symmetric cells, liquid-liquid (LL), liquid-gel (LG), gel-liquid (GL), and gel-gel (GG).

EIS data of four symmetric cells at various temperatures is shown in Fig 19. LL and LG with LE formation were measured higher resistance than GL and GG.  $R_{sei}$  of LL is higher than that of LG, and  $R_{ct}$  of LL varies widely as temperature changes compared to that of LG. In case of GL and GG,  $R_{sei}$  of both of them are similar to each other since both cells have polymer layer.  $R_{ct}$  of them also have similar tendency due to the same rea-

son.

From the result calculated by change of  $R_{ct}$ , de-solvation energy is listed as  $LL > LG = GG > GL$ . This is against my expectation that de-solvation energy of LG, GL, and GG would not differ from one another (Fig 20). Since polymer layer exists only on the surface of electrode in case of GL unlike LG and GG, which is close to structure of polymer electrode coating process, GL might have advantages of both LE and polymer coating.



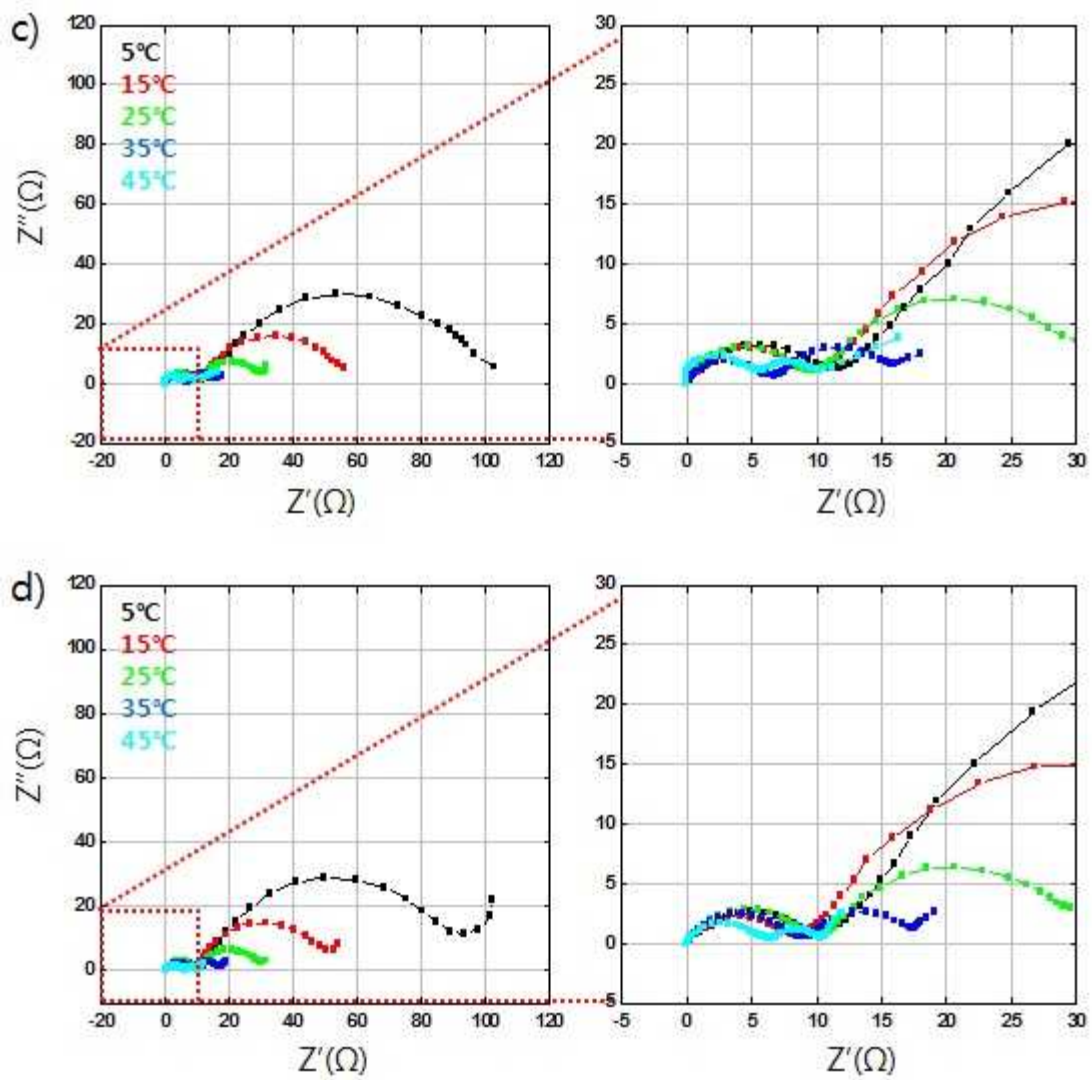


Fig 19. Temperature dependence of EIS data with coin symmetric cell,  
 a)liquid-liquid, b)liquid-gel, c)gel-liquid, and d)gel-gel

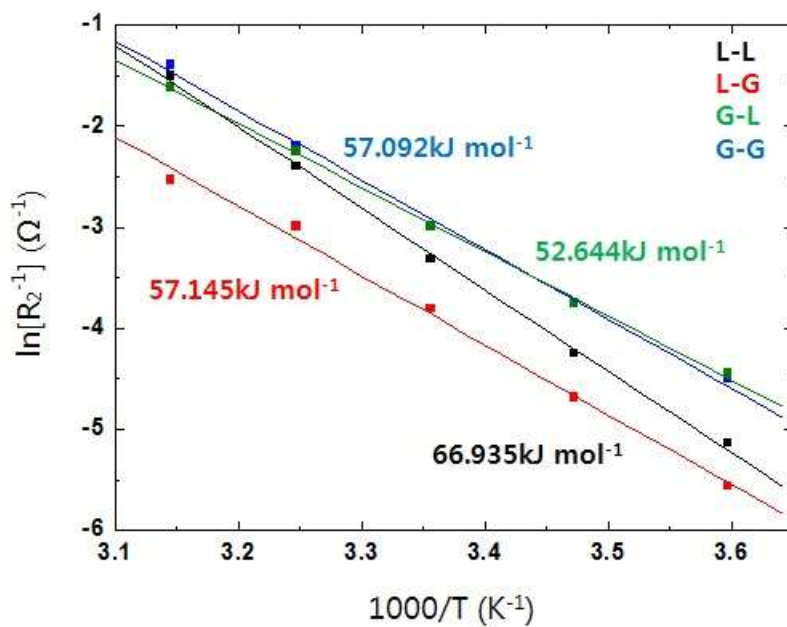


Fig 20. Temperature dependence of interfacial resistance of coin cathode symmetric cell  
GPE and Liquid electrolyte

#### 4.6. Effect of separator types on rate performance using $\text{LiNi}_{1/3}\text{Co}_{1/3}\text{Mn}_{1/3}\text{O}_2$ and Graphite

To consider the effects of separator on rate performance, coin  $\text{LiNi}_{1/3}\text{Co}_{1/3}\text{Mn}_{1/3}\text{O}_2$  half cell and coin full cell rate performance test had done using four types of separators, Celgard 2320 and Celgard C500 are manufactured by dry process, and Tonen and Asahi ND420 are manufactured by wet process.

In case of GPE, performance is listed as Tonen > Asahi ND420 > Celgard 2320 = Celgard C500. And in case of LE performance is listed as Tonen > Asahi ND420 > Celgard 2320 > Celgard C500 (Fig 21).

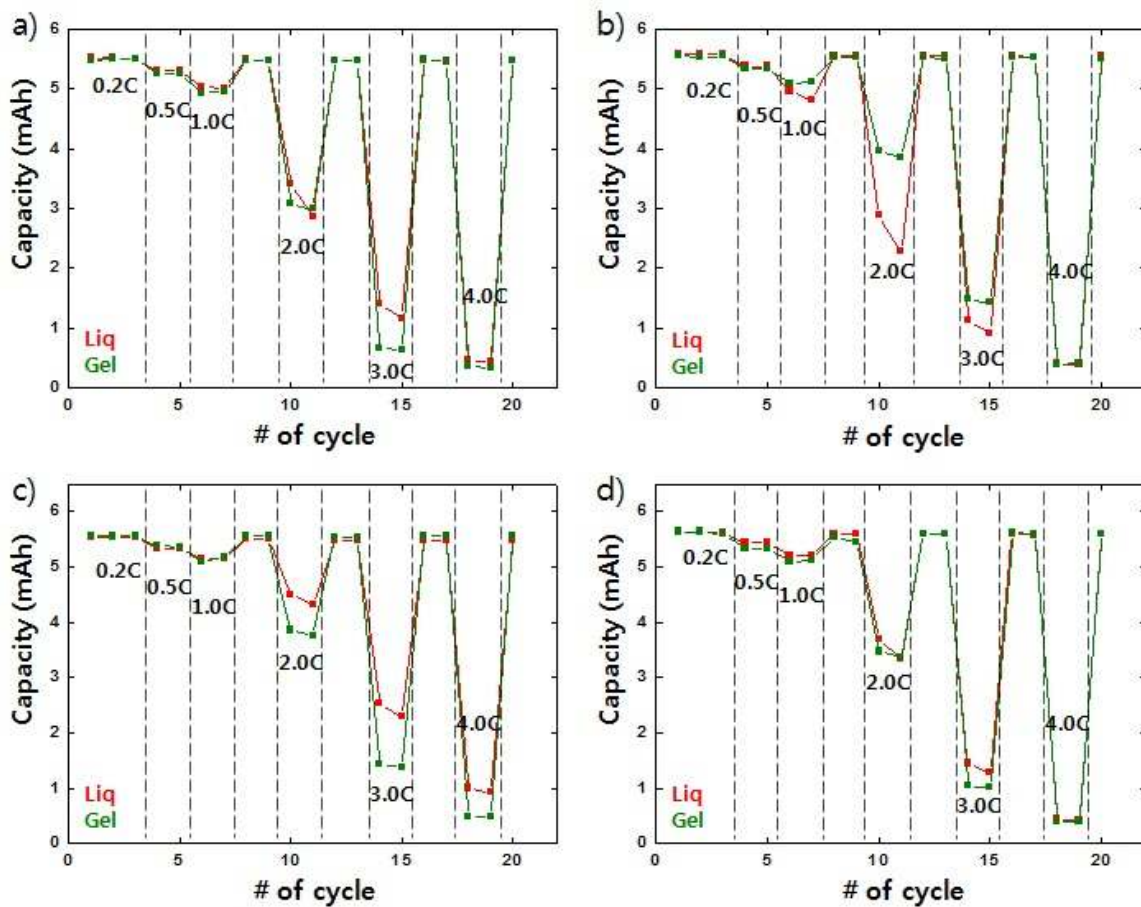


Fig 21. The  $\text{LiNi}_{1/3}\text{Co}_{1/3}\text{Mn}_{1/3}\text{O}_2$ /lithium foil coin cell discharge capacity at each rate  
a)Celgard C500, b)Celgard 2320, c)Tonen, and d)Asahi ND420

Since Celgard 2320 made by dry process and Tonen made by wet process showed better performance on half cell test, rate performance test of coin full cell had done using those two separators (Fig 22). In case of Tonen separator, little difference is observed between LE and GPE with regard to discharge capacity for each rate. However, discharge capacity of GPE is better than that of LE in case of Celgard2320. Regarding different separator in same electrolyte, both separators have no difference in rate performance in GPE. However, in case of LE, the discharge capacity of coin full cell using Celgard 2320 decreased after 1.0C while the rate performance of cell using Tonen separator maintained well.

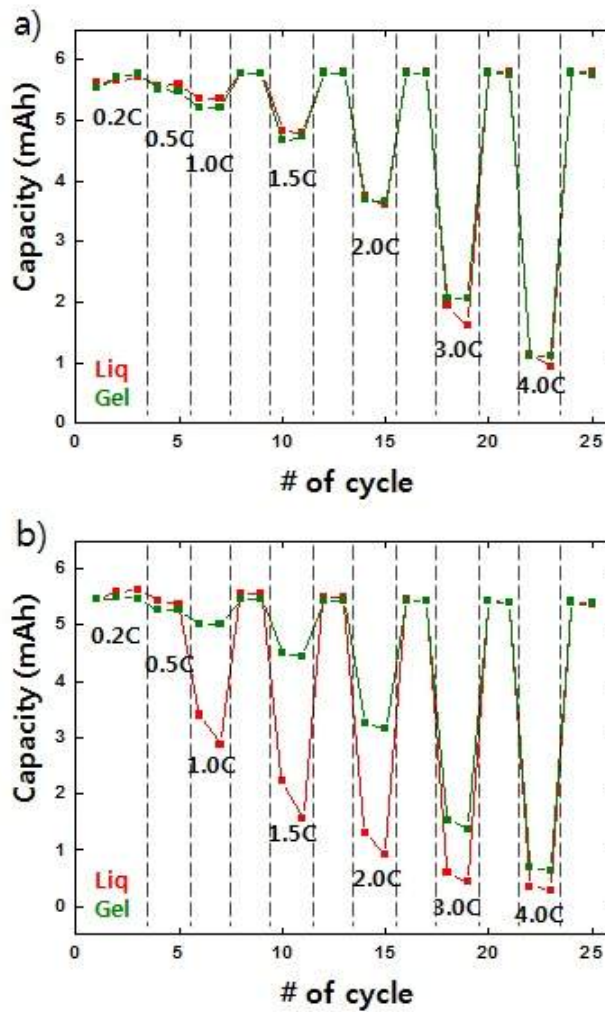


Fig 22. The  $\text{LiNi}_{1/3}\text{Co}_{1/3}\text{Mn}_{1/3}\text{O}_2/\text{Graphite}$  coin cell discharge capacity at each rate  
 a) Tonen, and b) Celgard 2320

Separators are different in pore size, ionic conductivity, and manufacturing process of dry type or wet type. LE is very different in c-rate discharge capacity by type of separator, because c-rate performance is influenced by characteristic of each separator. However, GPE has coated on the separator, its surface and pore. Thus, performance of GPE depends on the characteristic of GPE, not separator properties.

#### 4.7. $\text{LiNi}_{0.5}\text{Co}_{0.2}\text{Mn}_{0.3}\text{O}_2/\text{Graphite}$ and $\text{LiCoO}_2/\text{Graphite}$ coin full cell test using two type separators

$\text{LiNi}_{0.5}\text{Co}_{0.2}\text{Mn}_{0.3}\text{O}_2$  and  $\text{LiCoO}_2$  cathode materials were used for experiment to know the influence of cathodes. Fig 23 shows the results of rate performance using  $\text{LiNi}_{0.5}\text{Co}_{0.2}\text{Mn}_{0.3}\text{O}_2$ . Rate performance is higher than  $\text{LiNi}_{1/3}\text{Co}_{1/3}\text{Mn}_{1/3}\text{O}_2$  because capacity is smaller. Fig 23a) with Tonen separator, shows that GPE discharge

capacity is similar to LE. Fig 23b), with Celgard 2320 separator high rate (over 2.0C) discharge capacity of GPE is higher than that of LE.

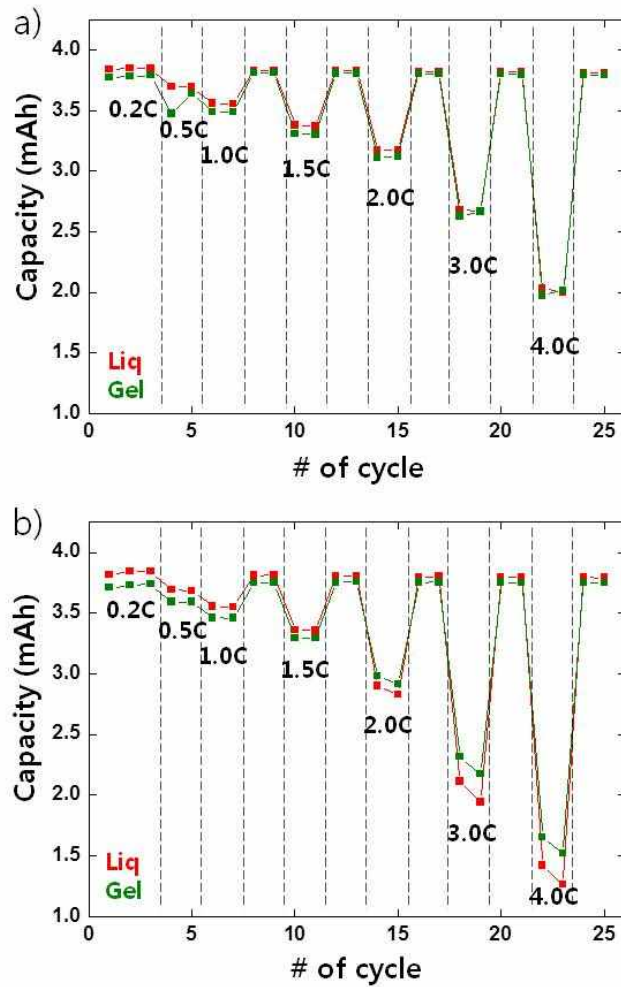


Fig 23. The  $\text{LiNi}_{0.5}\text{Co}_{0.2}\text{Mn}_{0.3}\text{O}_2/\text{Graphite}$  coin cell discharge capacity at each rate  
a) Tonen, and b) Celgard 2320

The rate performance of the cell using  $\text{LiCoO}_2$  is shown in Fig 24. The rate performance of  $\text{LiCoO}_2$  is similar to the using other cathode materials. Rate performance of LE seems slightly higher than that of GPE with Tonen using cell, rate performance of GPE was higher only with Celgard 2320.

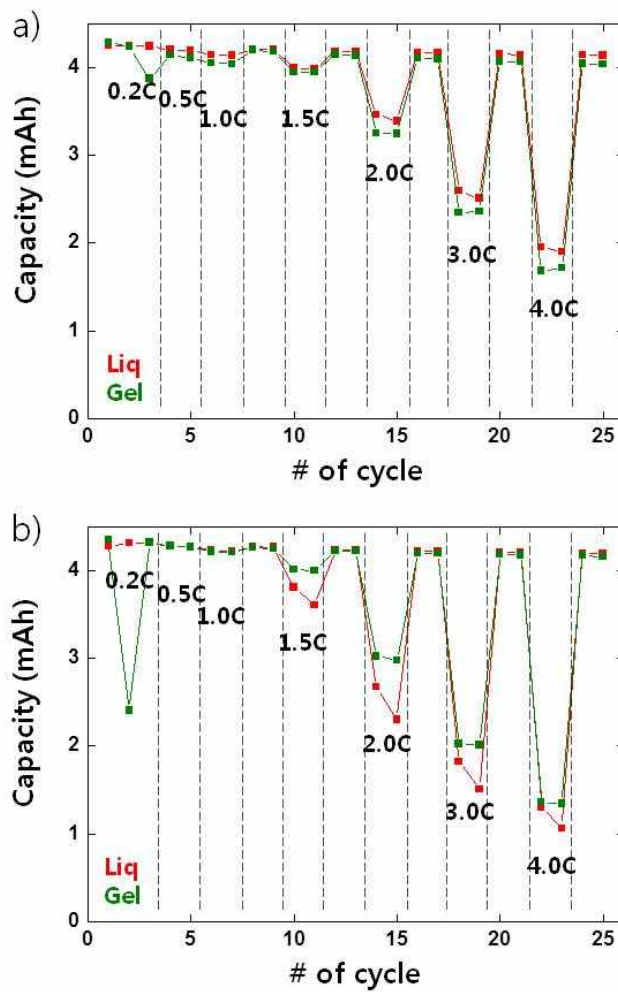


Fig 24. The LiCo<sub>2</sub>/Graphite coin cell discharge capacity at each rate a) Tonen, and b) Celgard 2320

Consequentially, rate performance curve showed similarly depending on the difference in separator, not the cathode. The reason for this is that SEI like layer formation on the electrode surface does not depend on components of the electrodes. Thus, rate performance does not depend on the cathodes because de-solvation process happens on the SEI like layer.

## V. Conclusion

This study demonstrates that the GPE prepared by using acrylate monomer exhibits higher energy density at high rate compared to the liquid type electrolyte. It was found that  $\text{LiNi}_{1/3}\text{Mn}_{1/3}\text{Co}_{1/3}\text{O}_2$ /graphite cell employing the GPE exhibits 60 % higher discharge capacity at 2 C rate than the cell with LEs, while both cells show similar capacity at 0.2 C discharge. The better power performance in the GPE was also confirmed for  $\text{LiNi}_{0.5}\text{Co}_{0.2}\text{Mn}_{0.3}\text{O}_2$  and  $\text{LiCoO}_2$  electrodes. Based on the Arrhenius plot of the interfacial impedance, the improved power performance in the GPE was ascribed to the lower activation energy of the GPE. The decreased activation energy seems to stem from diminished desolvation energy of  $\text{Li}^+$  ion in the GPE, which needs further study to be proven. It was also found that the power performance in the GPE is hardly affected by the type of separator in contrast to that in the liquid electrolyte.

## References

- [1] T. Sato, K. Banno, T. Maruo, R. Nozu. "New design for a safe lithium-ion gel polymer battery." *J. Power Sources*. 152 (2005) 254-271
- [2] M.M. Rao, J.S. Liu, W.S. Li, Y. Liang, D.Y. Zhou. "Preparation and performance analysis of PE-supported P(AN-co-MMA) gel polymer electrolyte for lithium ion battery application." *J. Membrane Sci.* 322 (2008) 314-319
- [3] T. Yamamoto, T. Hara, K. Segawa, K. Honda, H. Akashi. "4.4 V lithium-ion polymer batteries with a chemical stable gel electrolyte." *J. Power Sources*. 174 (2007) 1036-1040
- [4] Z. Chen, L.Z. Zhang, R. West, K. Amine. "Gel electrolyte for lithium-ion batteries." *Electrochim Acta*. 53 (2008) 3262-3266
- [5] Y.H. Liao, X.P. Li, C.H. Fu, R. Xu, M.M. Rao, L. Zhou, S.J. Hu, W.S. Li. "Performance improvement of polyethylene-supported poly(methyl methacrylate-vinyl acetate)-co-poly(ethylene glycol) diacrylate based gel polymer electrolyte by doping nano-Al<sub>2</sub>O<sub>3</sub>." *J. Power Sources*. 196 (2008) 6723-6728
- [6] B.E. Blomgren. *Lithium Batteries*, Academic Press, (1983) New York
- [7] M. Ue. "Solution Chemistry of Organic Electrolytes," *Prog. Batteries Battery Materials*. 16 (1997) 332-349.
- [8] K. Araki, N. Sato. "Chemical transformation of the electrode surface of lithium-ion battery after storing at high temperature." *J. Power Sources*. 124 (2003) 124-132
- [9] F. Kita, H. Sakata, S. Sinomoto, A. Kawakami, H. Kamizori, T. Sonoda, H. Nagashima, J. Nie, N.V. Pavlenko, Y.L. Yagupolskii. "Characteristics of the electrolyte with fluoro organic lithium salts." *J. Power Sources*. 90 (2000) 27-32
- [10] P. Ping, Q. Wang, J. Sun, H. Xiang, and C. Chen. "Thermal Stabilities of Some Lithium Salts and Their Electrolyte Solutions With and Without Contact to a LiFePO<sub>4</sub> Electrode." *J. Electrochem. Soc.* 157 (11) (2010) A1170-A1176
- [11] D. Aurbach, K. Gamolsky, B. Markovsky, Y. Gofer, M. Schmidt, and U. Heider. "On the use of vinylene carbonate (VC) as an additive to electrolyte solutions for Li-ion batteries." *Electrochim Acta*. 47 (2002) 1423-1439
- [12] S.K. Jeong, M. Inaba, R. Mogi, Y. Iriyama, T. Abe, and Z. Ogumi. "Surface Film Formation on a Graphite Negative Electrode in Lithium-Ion Batteries: Atomic Force Microscopy Study on the Effects of Film-Forming Additives in Propylene Carbonate Solutions." *Langmuir*. 17 (2001) 8281-8286

- [13] J.R. Dahn, J. Jiang, L.M. Moshurchak, M.D. Fleischauer, C. Buhrmester, and L.J. Krause. "High-Rate Overcharge Protection of LiFePO<sub>4</sub>-Based Li-Ion Cells Using the Redox Shuttle Additive 2,5-Ditertbutyl-1,4-dimethoxybenzene." *J. Electrochem. Soc.* 152 (6) (2005) A1283-A1289
- [14] K. Shima, K. Shizuka, M. Ueb, H. Ota, T. Hatozaki, and J.I. Yamaki. "Reaction mechanisms of aromatic compounds as an overcharge protection agent for 4V class lithium-ion cells." *J. Power Sources.* 161 (2006) 1264–1274
- [15] G.S. Song, W.S. Lee, I.J. Lee, and D.H. Suh. "Solid Polymer Electrolytes for Secondary Lithium Batteries." *J.Korean Ind. Eng. Chem.* 13 (4) (2002) 297-308
- [16] J.R. MacCallum, C.A. Vincent. *Polymer Electrolyte Reviews, Vol.1 and 2*, Elsevier Applied Science, (1986, 1989) London
- [17] J.B. Bates, N.J. Dudney, G.R. Gruzalski, R.A. Zuhr, A. Choudhury, and C.F. Luck. "Fabrication and characterization of amorphous lithium electrolyte thin films and rechargeable thin-film batteries." *J. power Sources.* 103 (1993) 43-44
- [18] J. Fu. "Faast Li<sup>+</sup> ion Conduction in Li<sub>2</sub>O-Al<sub>2</sub>O<sub>3</sub>-TiO<sub>2</sub>-SiO<sub>2</sub>-P<sub>2</sub>O<sub>5</sub> Glass-Ceramics." *J. Am. Ceram. Soc.* 80 (1997) 1901-1903
- [19] M. Tatsumisago, H. Morimoto, H. Yamashita and T. Minami. "Preparation of amorphous solid electrolytes in the system Li<sub>2</sub>S–SiS<sub>2</sub>–Li<sub>4</sub>SiO<sub>4</sub> by mechanical milling." *Solid State Ionics.* 483 (2000) 136-137
- [20] R. Kanno and M. Maruyama, "Lithium Ionic Conductor Thio-LISICON: The Li<sub>2</sub>S-GeS<sub>2</sub>-P<sub>2</sub>S<sub>5</sub> System." *J. Electrochem. Soc.* 148 (2001) A742-A746
- [21] P.E. Stallworth, J.J. Fontanella, M.C. Wintersgill, C.D. Scheidler, J.J. Immel, S.G Greenbaum, and A.S. Gozdz. "NMR, DSC and high pressure electrical conductivity studies of liquid and hybrid electrolytes." *J. Power Sources.* 81 (1999) 739–747
- [22] A.M. Stephan. "Review on gel polymer electrolytes for lithium batteries." *Eur Polym J.* 42 (2006) 21–42
- [23] N. Muniyandi, N. Kalaiselvi, P. Periyasamy, R. Thirunakaran, B.R. babu, S. Gopukumar, T. Premkumar, N.G. Renganathan, and M. Raghavan. "Optimisation of PVdF-based polymer electrolytes." *J. Power Sources.* 96 (2001) 14-19
- [24] K.H. Lee, H.S. Lim, and J.H. Wang. "Effect of unreacted monomer on performance of lithium-ion polymer batteries based on polymer electrolytes prepared by free radical polymerization." *J. Power Sources.* 139. (2005) 284–288
- [25] H.S. Kim, S.I. Moon, and S.P. Kim. "A Study on the Characteristics of Lithium-Ion Polymer Battery with Composition of Crosslink-Type Gel Polymer Electrolyte." *J. Electrochem. Soc. Kr.* 7 (4) (2004) 189-193
- [26] M.H. Ryou, Y.M. Lee, J.K. Park, and J.W. Choi. "Mussel-Inspired Polydopamine-Treated Polyethylene

Separators for High-Power Li-Ion." *Adv. Mater.* 23 (2011) 3066–3070

[27] S.K. Kim, B.J. Shin, J.H. Kim, S. Ahn, S.Y. Lee. "Nano-encapsulation of graphite-based anodes by a novel polymer electrolyte and its influence on C-rate performances of Li-ion batteries." *Electrochem. Commun.* 10 (2008) 1625–1628

[28] Y. Li and P.S. Fedkiw. "Rate Capabilities of Composite Gel Electrolytes Containing Fumed Silica Nanoparticles." *J. Power Sources.* 153 (11) (2006) A2126-A2132

[29] T. Abe, F. Sagane, M. Ohtsuka, Y. Iriyama, and Z. Ogumi. "Lithium-Ion Transfer at the Interface Between Lithium-Ion Conductive Ceramic Electrolyte and Liquid Electrolyte-A Key to Enhancing the Rate Capability of Lithium-Ion Batteries." *J. Electrochem. Soc.* 152 (11) (2005) A2151-A2154

[30] T.R. Jow, M.B. Marx, and J.L. Allen. "Distinguishing Li<sup>+</sup> charge transfer kinetics at NCA/Electrolyte and Graphite/Electrolyte interfaces, and NCA/Electrolyte and LFP/Electrolyte Interfaces in Li-ion cells." *J. Electrochem. Soc.* 159 (5) (2012) A604-A612

[31] Y. Yamada, Y. Iriyama, T. Abe, and Z. Ogumi. "Kinetics of Lithium Ion Transfer at the Interface between Graphite and Liquid Electrolytes: Effects of Solvent and Surface Film." *Langmuir.* 25 (21) (2009) 12766–12770

[32] M. Kaneko, M. Nakayama, Y. Wakizaka, and K. Kanamura, and M. Wakihara. "Enhancement of electrochemical ion/electron-transfer reaction at solid|liquid interface by polymer coating on solid surface." *Electrochim Acta.* 53 (2008) 8196–8202

[33] B. Baek, and C.I. Jung. "Enhancement of the Li<sup>+</sup> ion transfer reaction at the LiCoO<sub>2</sub> interface by 1,3,5-trifluorobenzene." *Electrochim Acta.* 55 (2010) 3307–3311

[34] N. Ogihara, S. Kawauchi, C. Okuda, Y. Itou, Y. Takeuchi, and Y. Ukyo. "Theoretical and Experimental Analysis of Porous Electrodes for Lithium-Ion Batteries by Electrochemical Impedance Spectroscopy Using a Symmetric Cell." *J. Electrochem. Soc.* 159 (7) (2012) A1034-A1039

[35] T.S. Ong, and H. Yang. "Symmetrical Cell for Electrochemical AC Impedance Studies of Lithium Intercalation into Graphite." *Electrochem. Solid St.* 4 (7) (2001) A89-A92

[36] C.H. Chen, J. Liu, and K. Amine. "Symmetric cell approach towards simplified study of cathode and anode behavior in lithium ion batteries." *Electrochem. Commun.* 3 (2001) 44-47

[37] C.H. Chen, J. Liu, and K. Amine. "symmetric cell approach and impedance spectroscopy of high power lithium-ion batteries." *J. Power Sources.* 96 (2001) 321-328

[38] K. Nakura, Y. Ohsugi, M. Imazaki, K. Ariyoshi, and T. Ohzuku. "Extending Cycle Life of Lithium-Ion Batteries Consisting of Lithium Insertion Electrodes: Cycle Efficiency Versus Ah-Efficiency." *J. Electrochem. Soc.* 158 (12) (2011) A1243-A1249

## 요 약 문

### 액체형 전해액의 출력 특성을 증가하는 아크릴레이트계 젤 고분자 전해액

본 논문은 안전성과 안정성이 높은 배터리의 개발을 위한 방법 중 젤 고분자 전해액을 사용하여 액체 전해액과 차이를 비교한 내용에 대해 다룬다. 아크릴레이트 계의 내부 열중합 방법을 사용하여 젤 고분자 전해액이 들어간 코인전지를 제조하고 출력 특성을 평가하여 액체 전해액 코인전지와 비교하였다. 일반적으로 알려져 있는 사실과 다르게 젤 고분자 전해액에서 약 30% 향상된 출력 특성을 얻을 수 있었다. 이런 출력 특성이 어떠한 전극에서 더 많은 영향을 주는지에 대해 조사하기 위해 양극과 음극 각각의 반쪽 코인 전지를 제조하여 측정하였고 그 중에서 양극에서의 영향이 더 크다는 것을 알 수 있었다. 이런 현상을 설명하기 위해서 전기화학적 임피던스 분광법(EIS)을 사용하여 전극과 전해액 계면 사이에서 일어나는 반응에 대해 알아보았다. 온도를 증가시키면서 EIS 를 측정하여 전극과 전해액 사이에서 리튬 이온의 출입 시에 필요한 de-solvation 에너지를 계산하였다. 젤 고분자 전해액 62kJ/mol 을 액체 고분자 전해액은 80kJ/mol 으로 계산되었다. 결과적으로 젤 고분자 전해액은 액체 고분자 전해액에 비해 낮은 de-solvation 에너지를 가지고 있고 이로 인하여 더 좋은 출력특성을 얻을 수 있는 것으로 해석된다. 또한 젤 고분자 전해액을 사용할 경우 분리막의 영향을 보기 위해 여러 종류의 분리막을 사용하여 실험을 진행하였다. 젤 고분자 전해액의 경우 분리막에 따른 차이가 없었지만 액체 전해액의 경우는 습식형에서는 좋은 출력특성을 건식형에서는 비슷한 출력특성을 볼 수 있었다.  $\text{LiCoO}_2$  와  $\text{LiNi}_{0.5}\text{Co}_{0.2}\text{Mn}_{0.3}\text{O}_2$  양극물질을 사용한 실험 결과 전극의 경우에는 출력특성에 큰 영향을 주지 않는다는 것을 알 수 있었다.

핵심어: 배터리, 젤 폴리머 전해액, 출력 특성, de-solvation 에너지

# Curriculum Vitae

Name: Dong Hui Kim

Birth Date: 1986. 08. 30

## Education

2005-2010 B.S., Department of Chemistry, KAIST

2011-2013 M.S., Department of Energy Systems Engineering, DGIST

## Presentation

Dong-Hui Kim, Sunghoon Yu, Jongho Jeon, Doo-Kyung Yang, and Hochun Lee "Synthesis and Characterization of Acrylate-based Gel Polymer Electrolyte for Li-ion Batteries" Presented at International Meeting on Lithium Batteries, ICC Jeju, Korea June 21, 2012